Ocean-Ice Interactions:

Antarctica & Greenland,
Theory & Observations

Keck Institute for Space Studies
September 9, 2013

David HOLLAND
New York University + Abu Dhabi

0

Overview:

Ocean-Ice Interface

Delivery of Water Masses

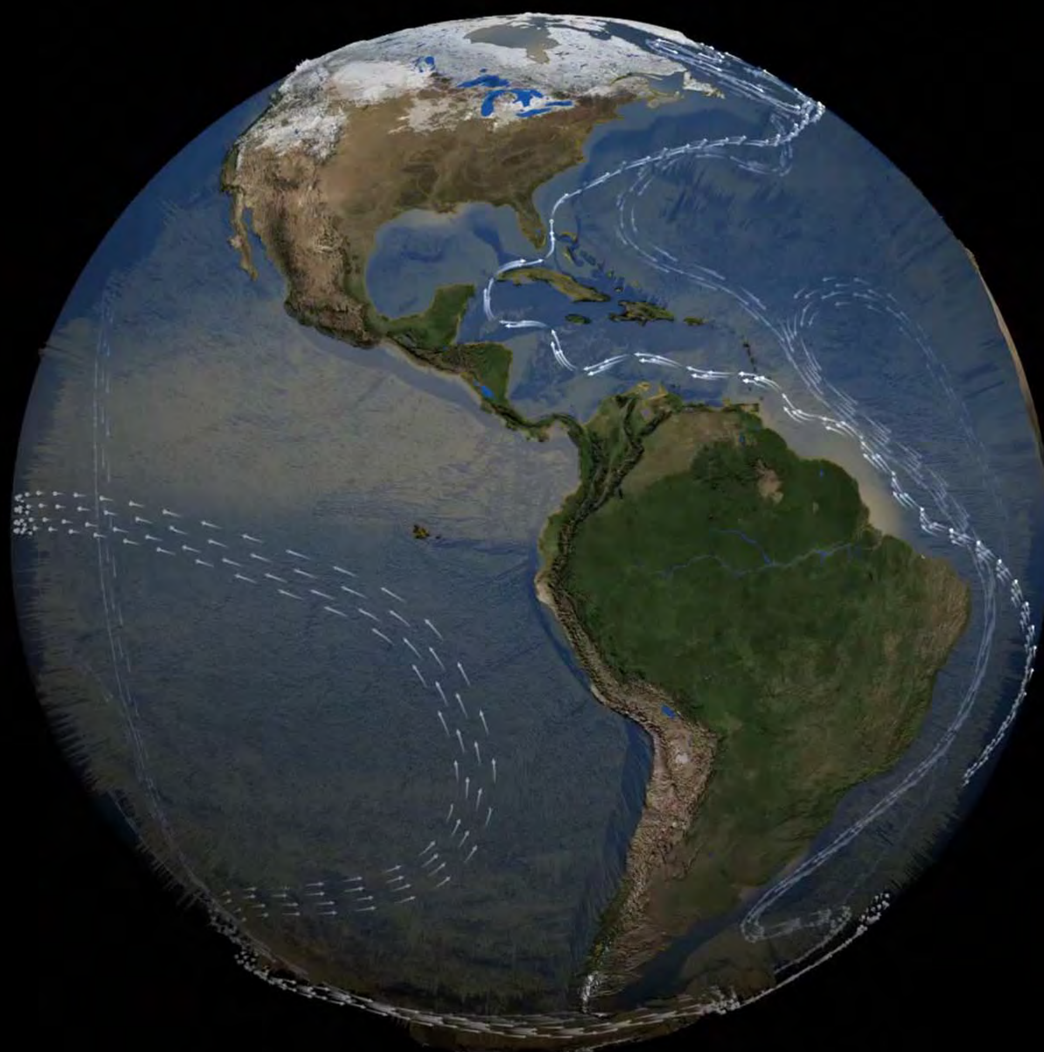

NASA

Scope of Interaction with Outlet Glaciers

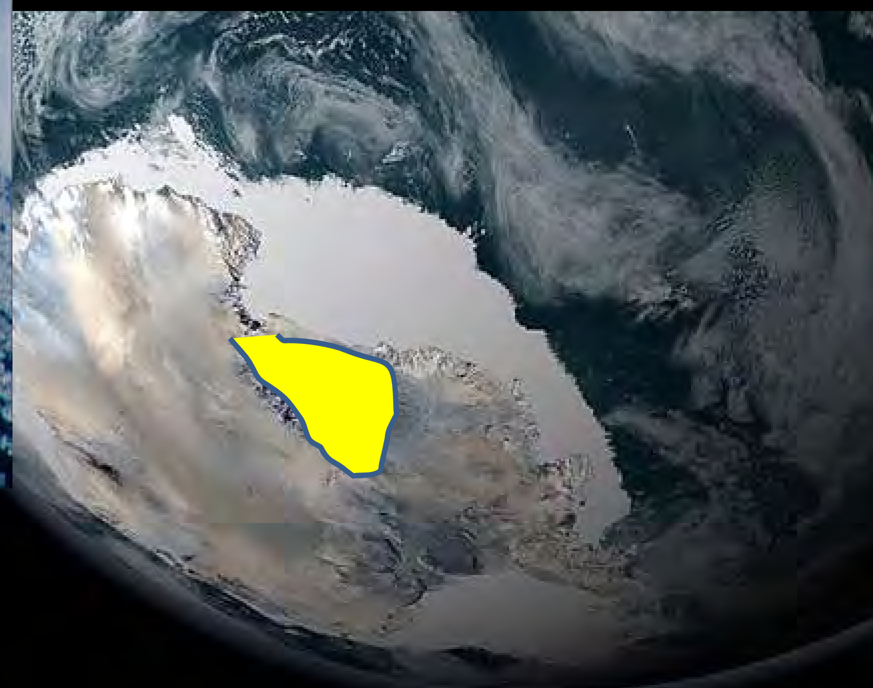

Prototypical Field Sites

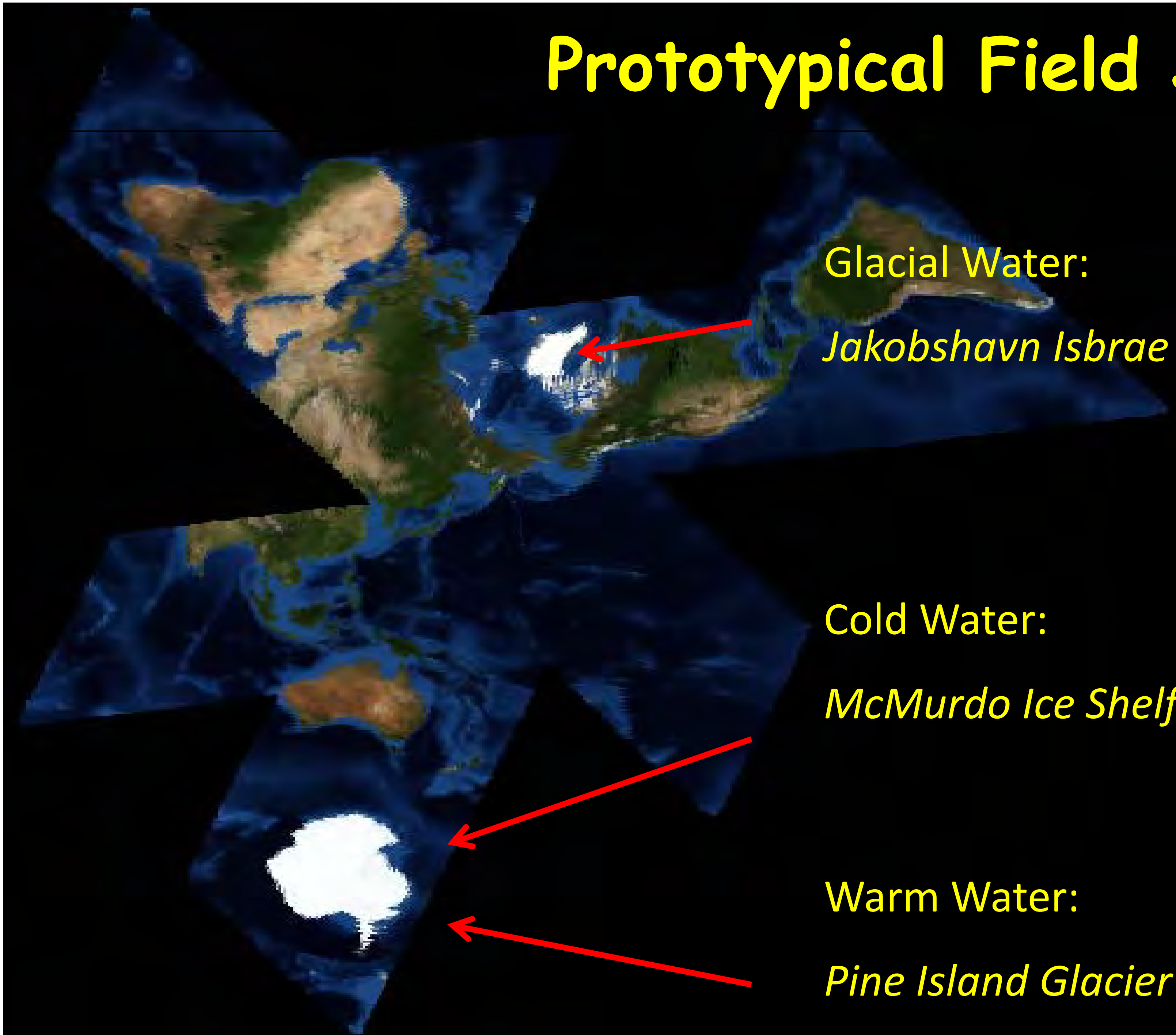

Glacial Water:

Jakobshavn Isbrae

Cold Water:

McMurdo Ice Shelf

Warm Water:

Pine Island Glacier

Google

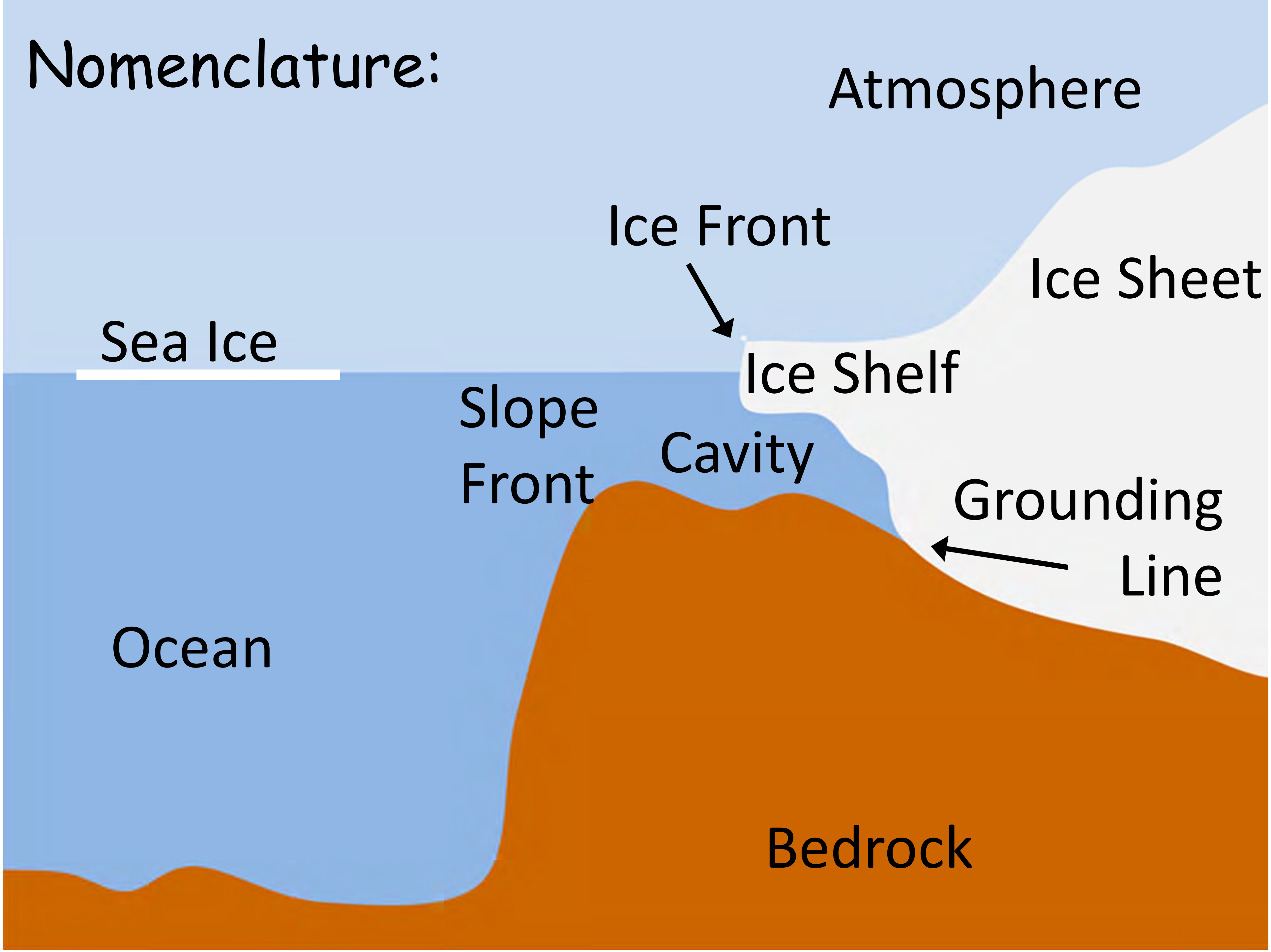
Nomenclature:
Atmosphere
Ice Front
Ice Sheet
Sea Ice
Ice Shelf
Slope Front
Cavity
Grounding Line
Ocean
Bedrock

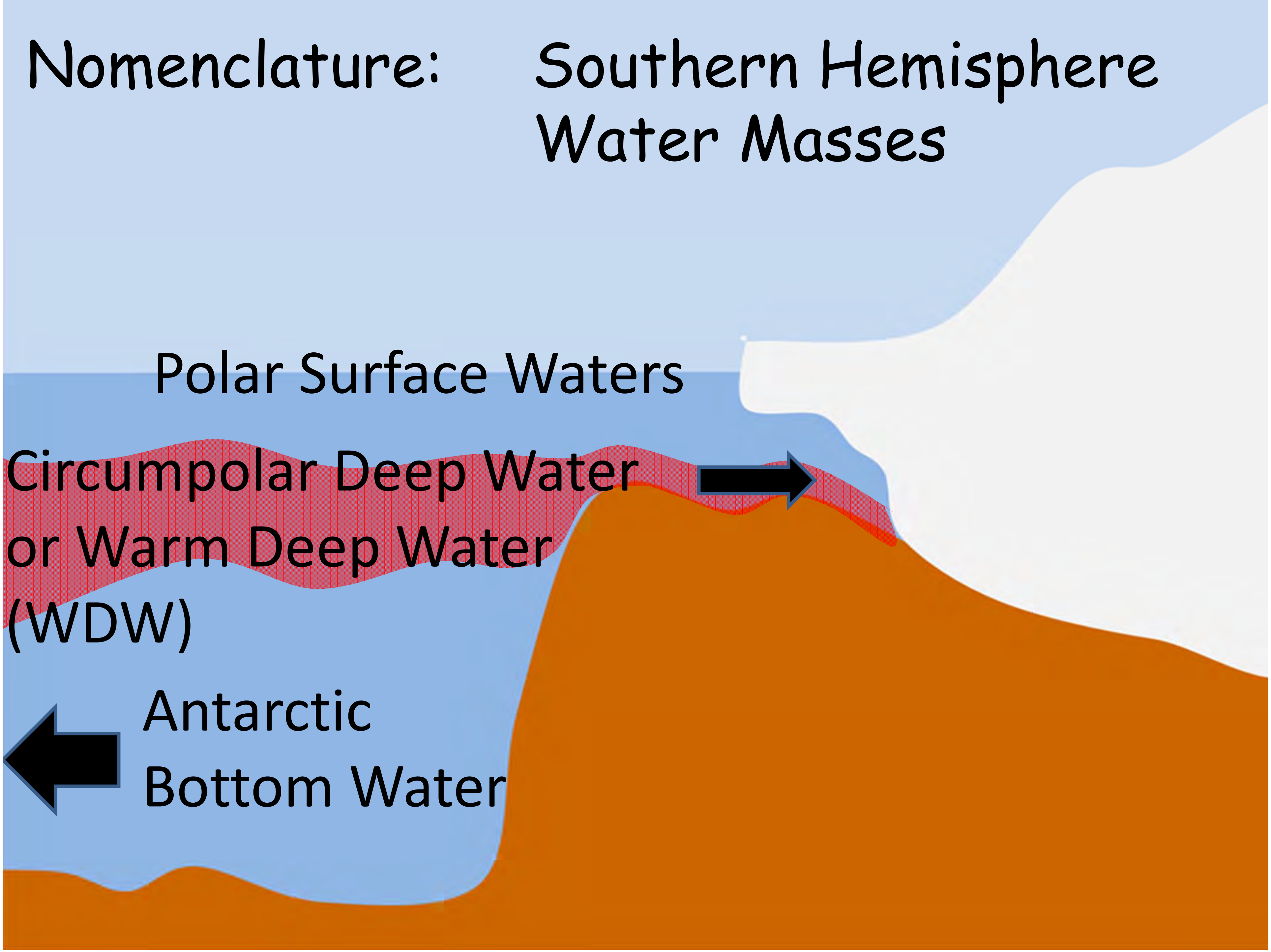

Nomenclature:
Southern Hemisphere Water Masses
Polar Surface Waters
Circumpolar Deep Water or Warm Deep Water (WDW)
Antarctic Bottom Water

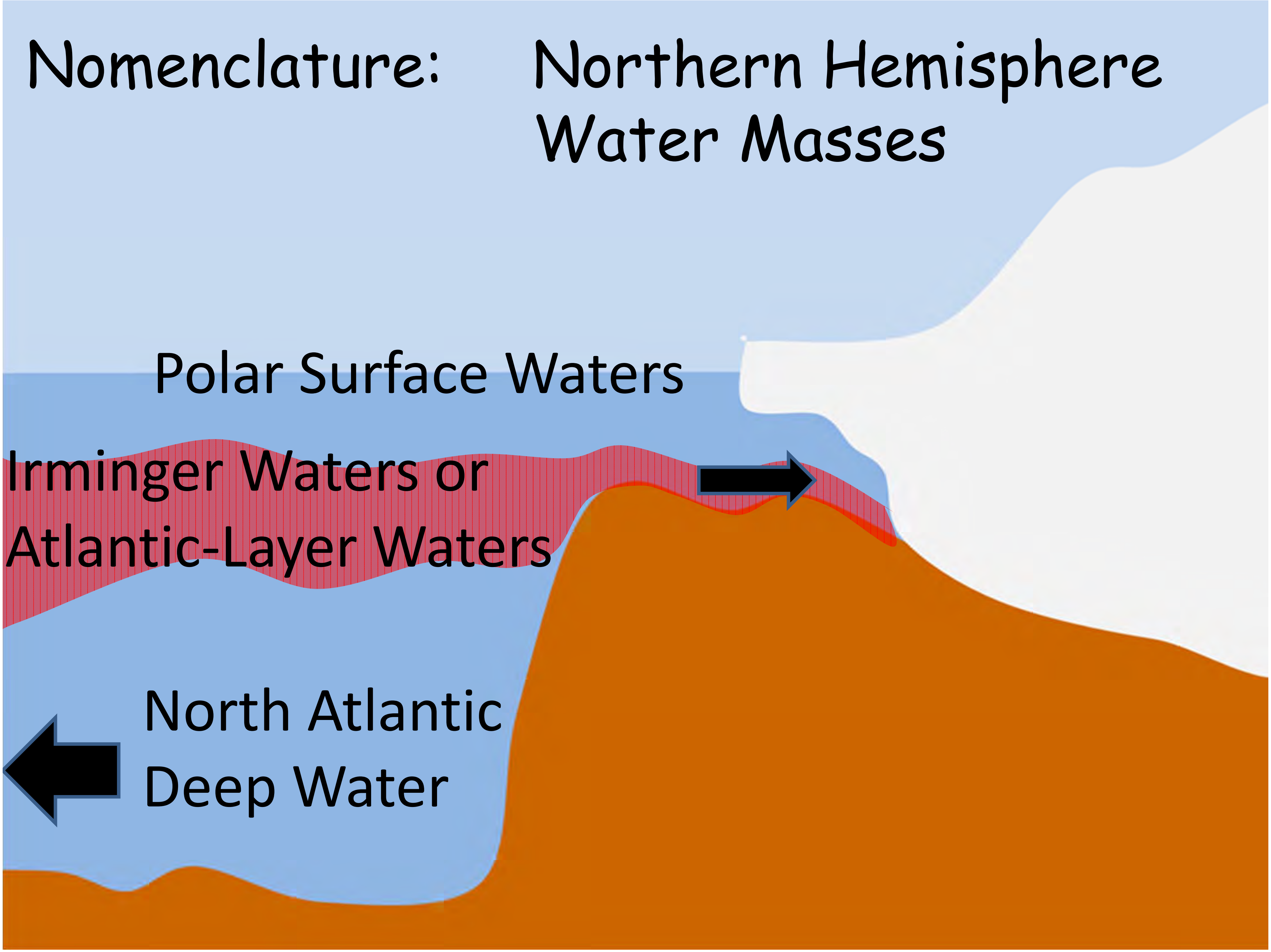
Nomenclature:
Northern Hemisphere
Water Masses
Polar Surface Waters
Irminger Waters or
Atlantic-Layer Waters
North Atlantic
Deep Water

Nomenclature: Continental Shelf Water Masses

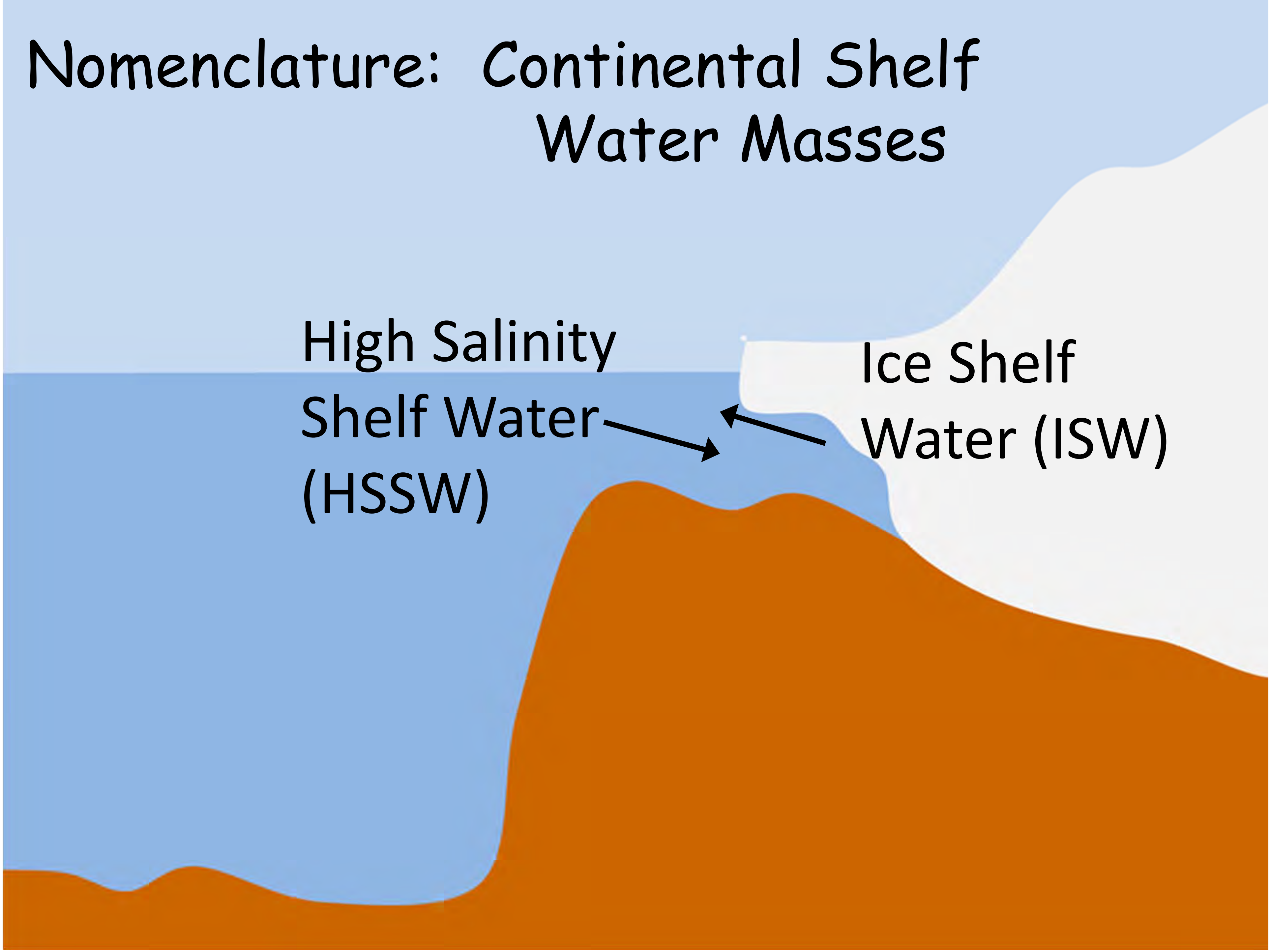

Nomenclature: Glacial Hydrology

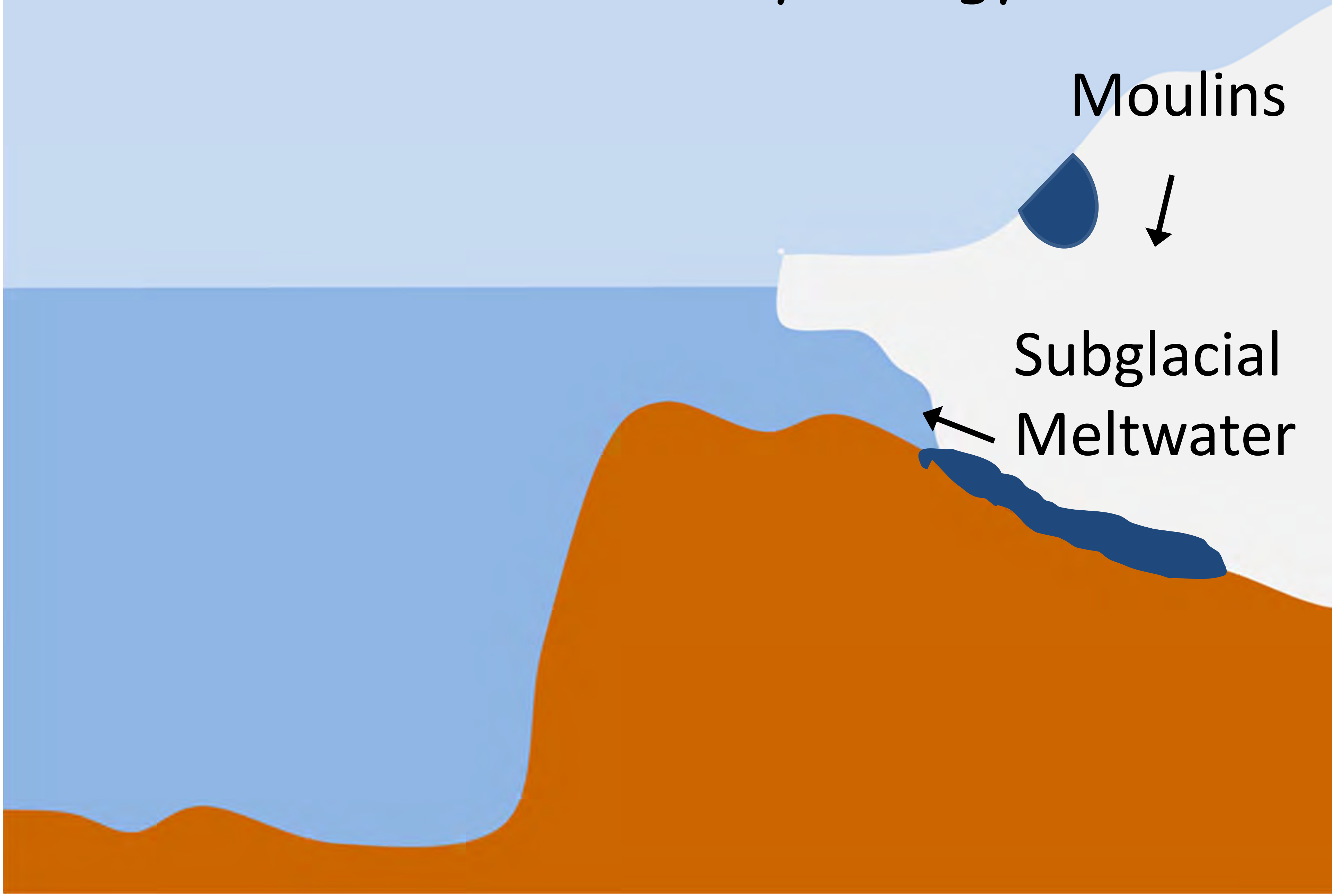

Primary Objective:
Position of the Ocean-Ice Interface

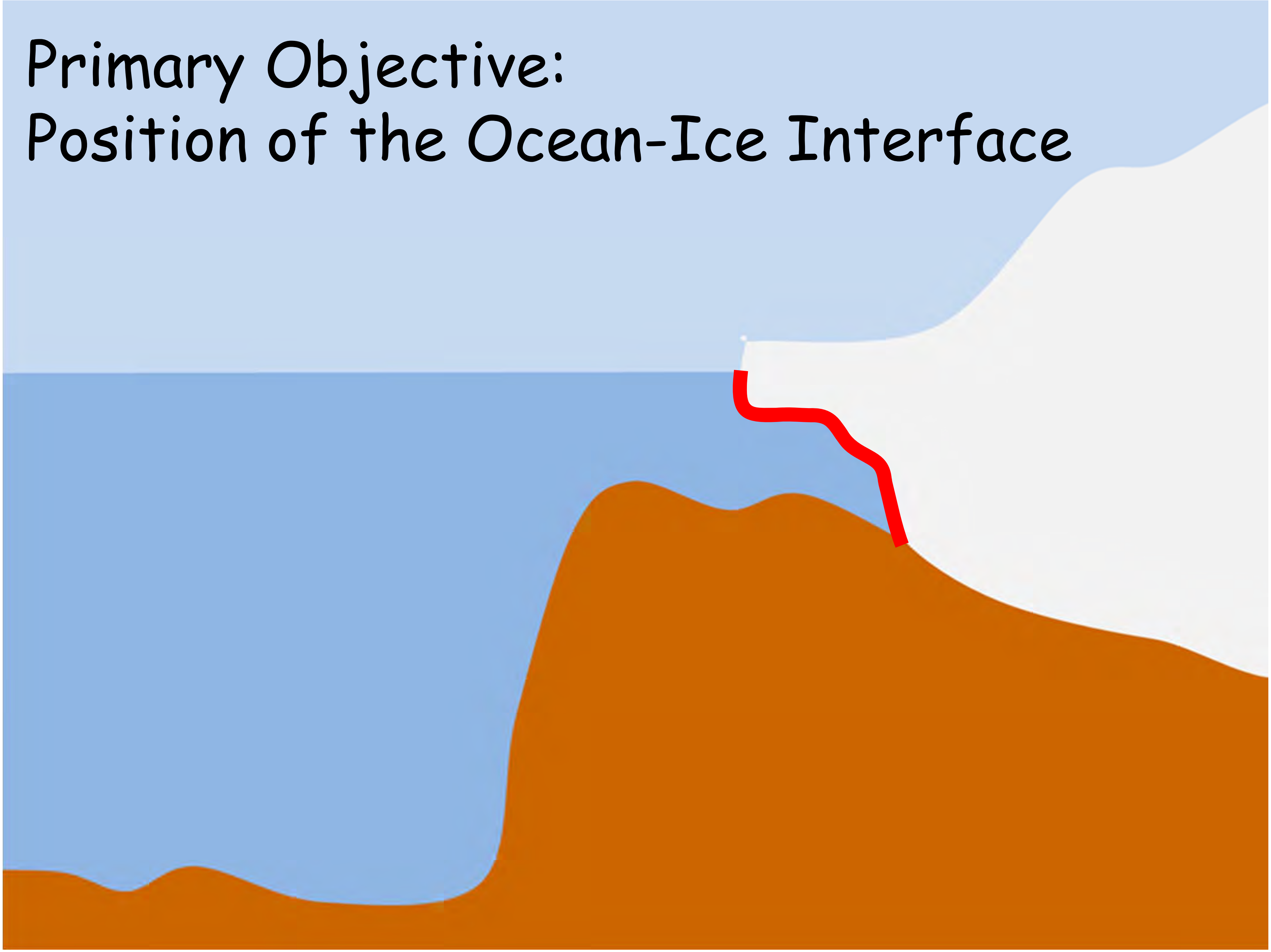

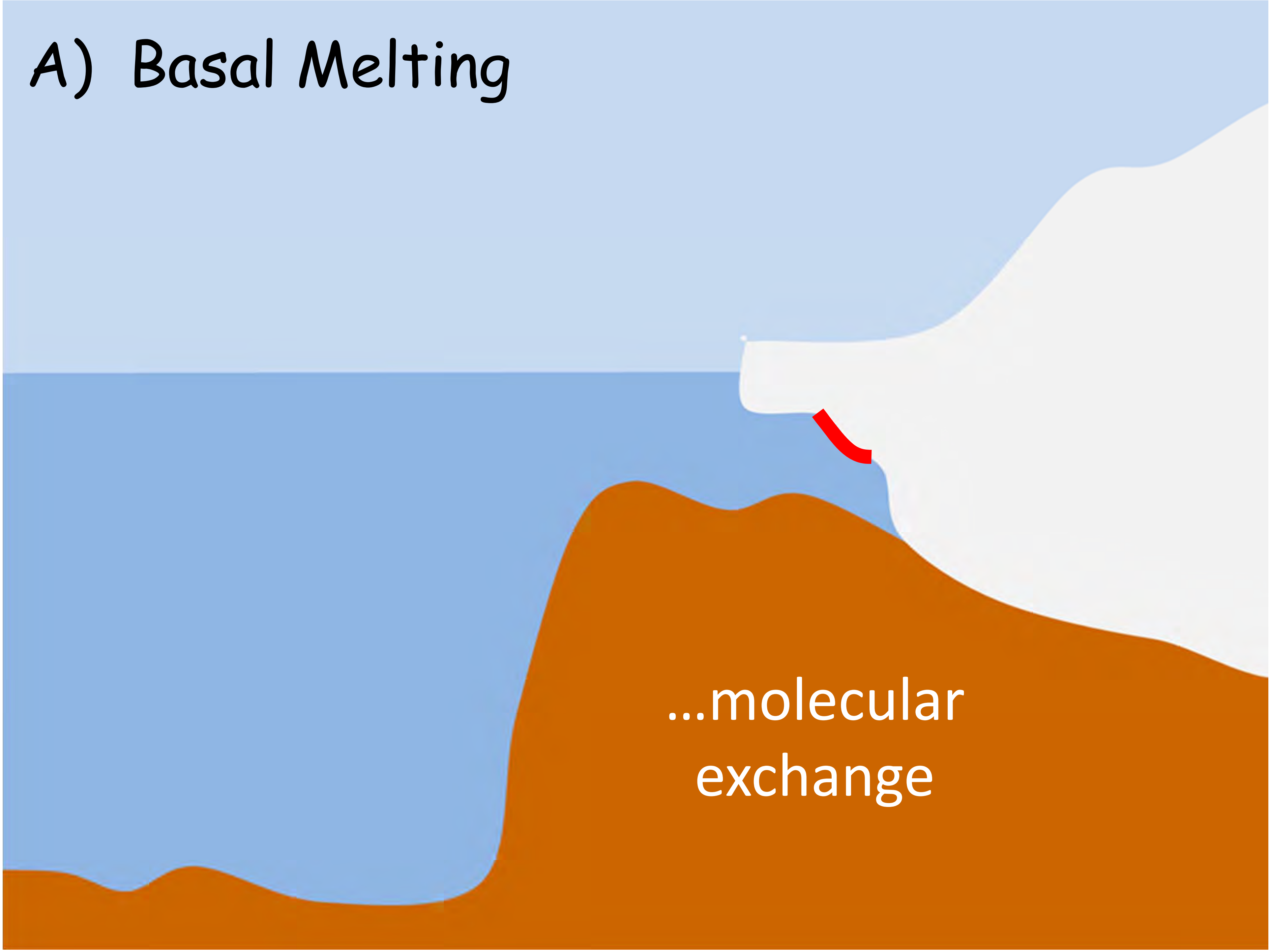
A) Basal Melting
…molecular
exchange

Three Modes of Basal Melting

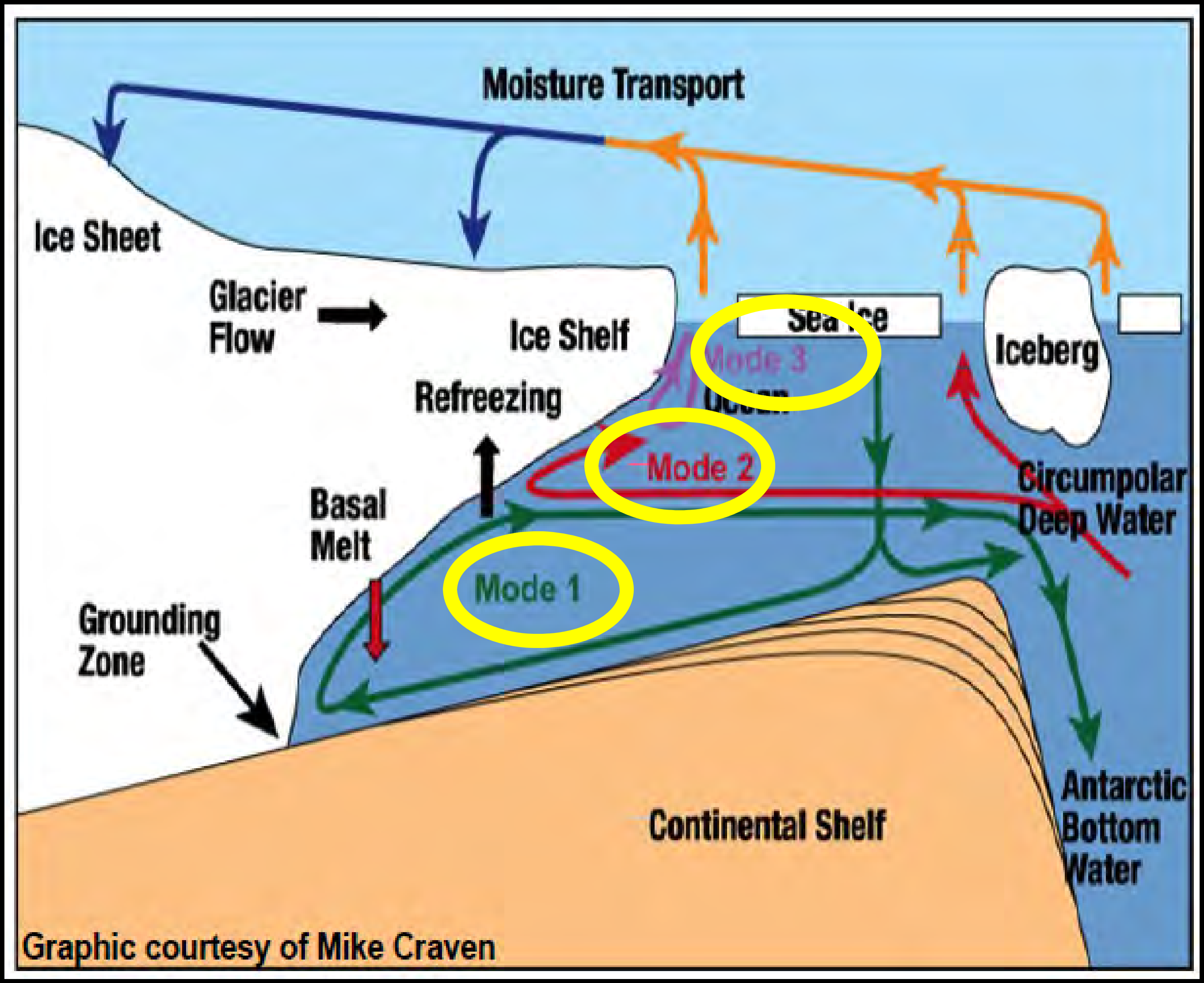

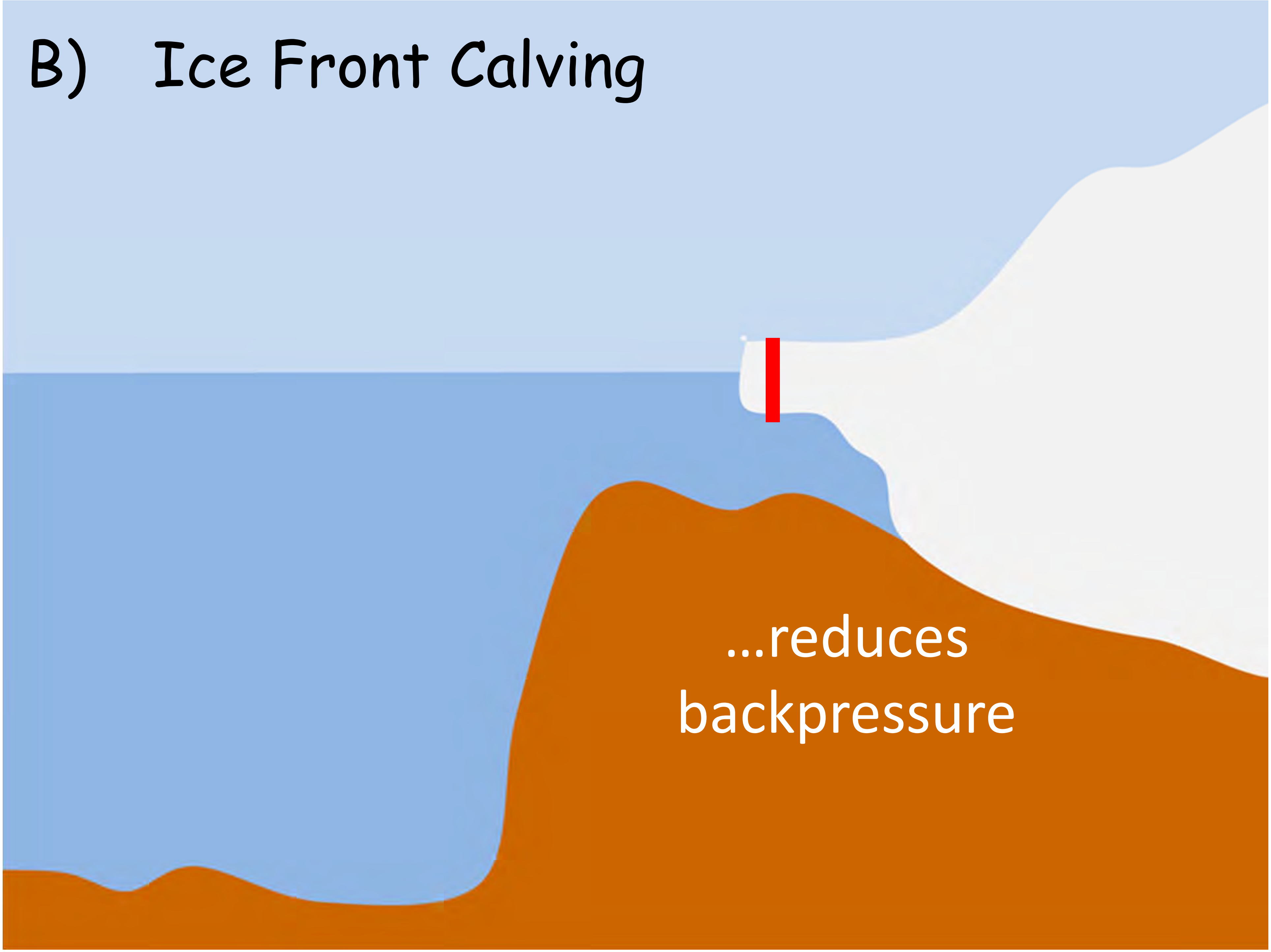
B) Ice Front Calving
...reduces
backpressure

A Mode of Ice Front Calving

Jakobshavn Isbræ, West Greenland
5 June 2007
14:10 - 14:28 UTC

photos by Jason Amundson
Geophysical Institute, University of Alaska Fairbanks

Ocean-Ice Melting:

Theoretical Background

Basal Melting: Viscous-Sublayer Model

Modeling Thermodynamic Ice–Ocean Interactions at the Base of an Ice Shelf

David M. Holland

Lamont-Doherty Earth Observatory, Palisades, New York

Adrian Jenkins

British Antarctic Survey, Cambridge, United Kingdom

(Manuscript received 6 May 1998, in final form 14 August 1998)

ABSTRACT

Models of ocean circulation beneath ice shelves are driven primarily by the heat and freshwater fluxes that are associated with phase changes at the ice–ocean boundary. Their behavior is therefore closely linked to the mathematical description of the interaction between ice and ocean that is included in the code. An hierarchy of formulations that could be used to describe this interaction is presented. The main difference between them is the treatment of turbulent transfer within the oceanic boundary layer. The computed response to various levels of thermal driving and turbulent agitation in the mixed layer is discussed, as is the effect of various treatments of the conductive heat flux into the ice shelf. The performance of the different formulations that have been used in models of sub-ice-shelf circulation is assessed in comparison with observations of the turbulent heat flux beneath sea ice. Formulations that include an explicit parameterization of the oceanic boundary layer give results that lie within about 30% of observation. Formulations that use constant bulk transfer coefficients entail a definite assumption about the level of turbulence in the water column and give melt/freeze rates that vary by a factor of 5, implying very different forcing on the respective ocean models.

Holland & Jenkins, *JPO*, 1999

Heat Fluxes

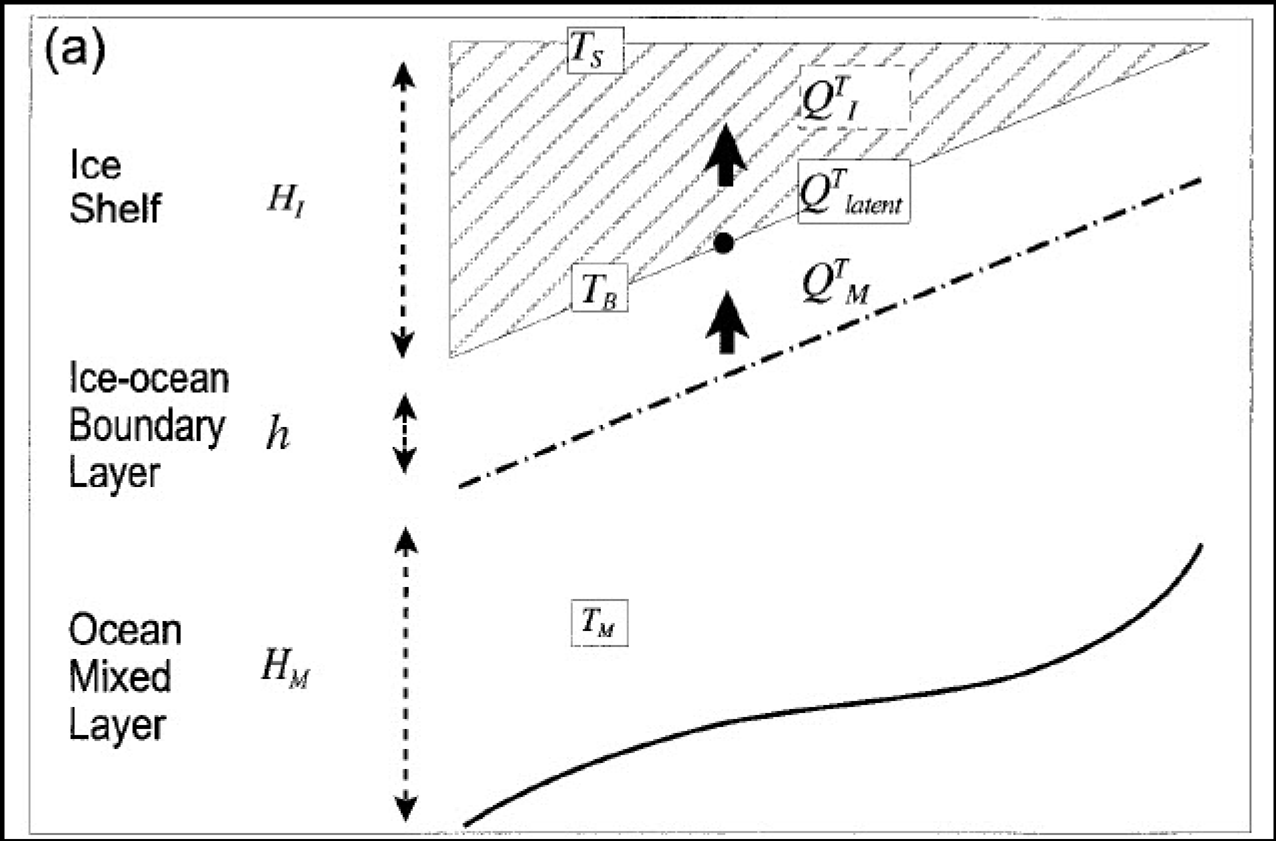

Holland & Jenkins, *JPO*, 1999

Viscous Sublayer

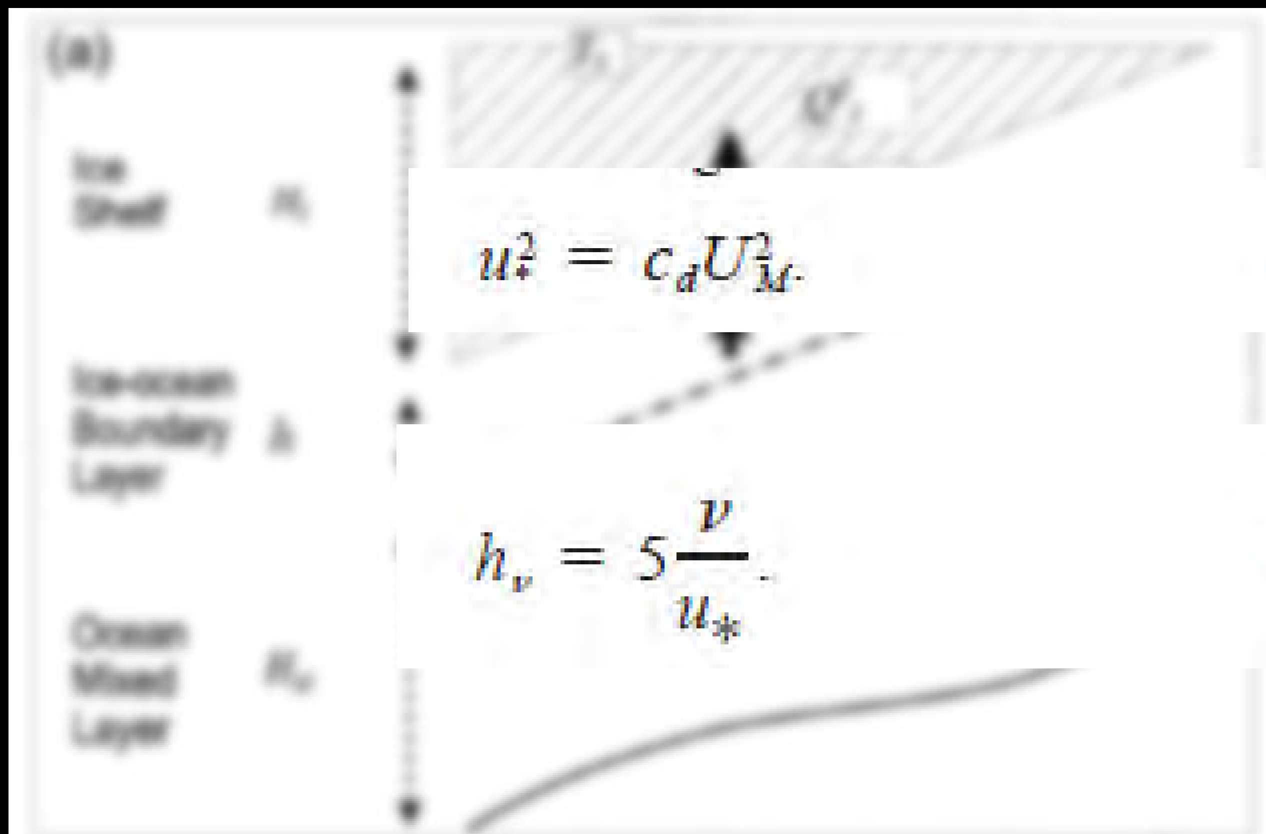

$$u_*^2 = c_d U_M^2. \qquad (13)$$

$$h_\nu = 5\frac{\nu}{u_*}. \qquad (17)$$

Holland & Jenkins, *JPO*, 1999

'One-Equation' Formulation

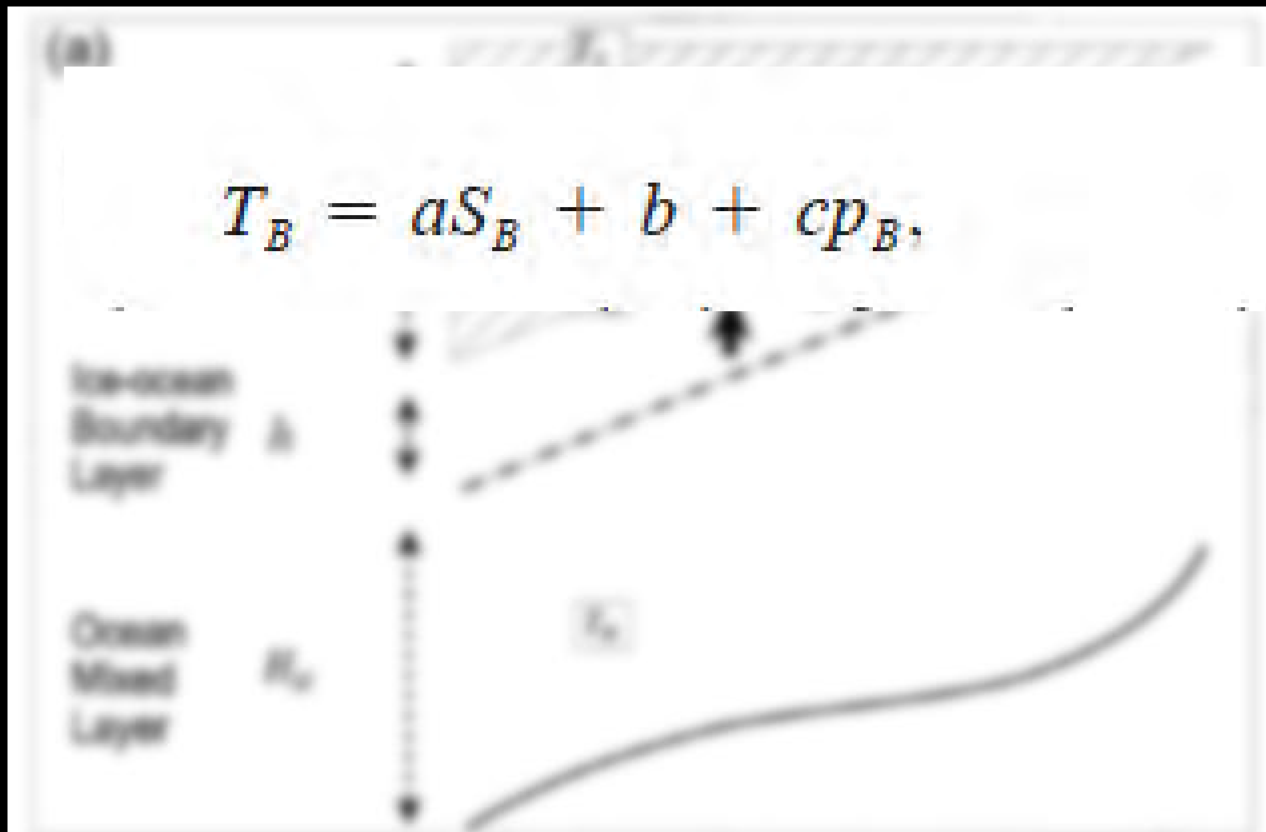

$$T_B = aS_B + b + cp_B, \qquad (1)$$

Holland & Jenkins, *JPO*, 1999

'Two-Equation' Formulation

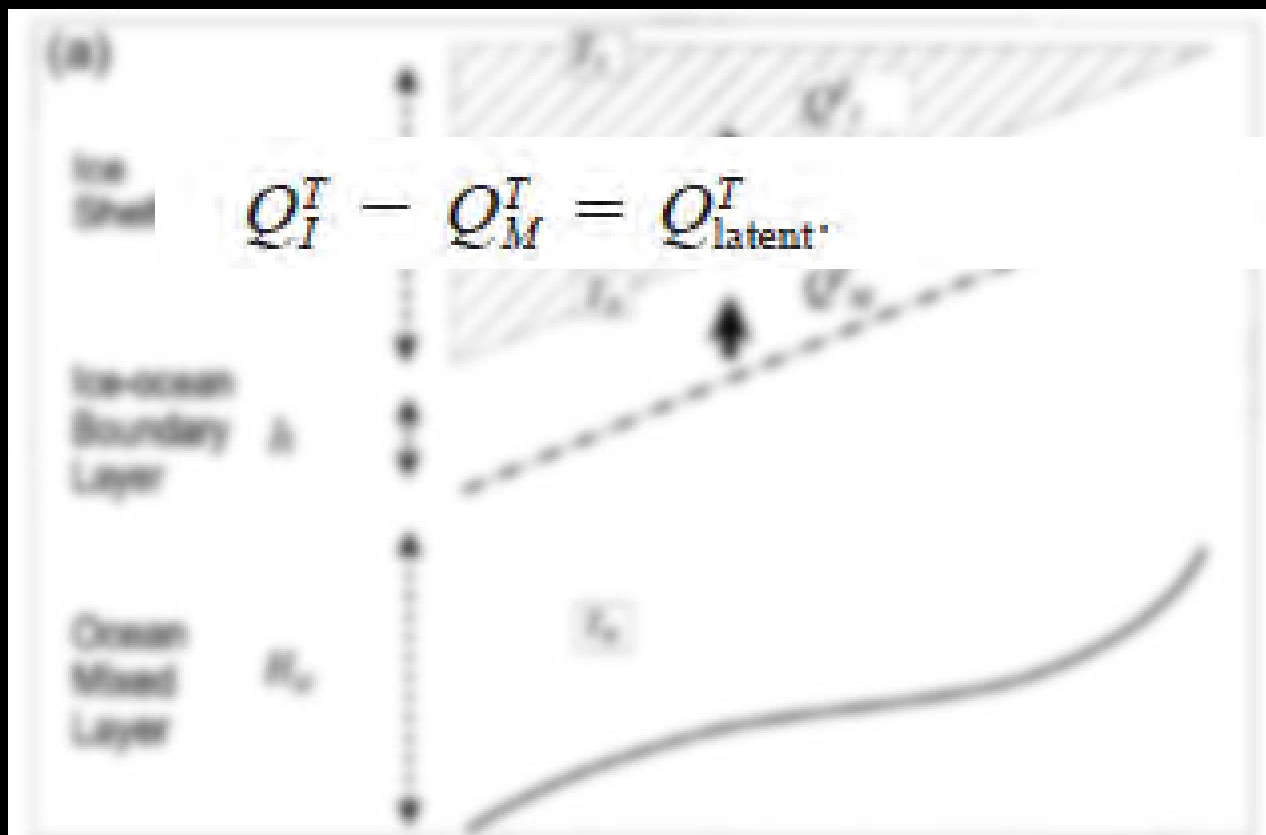

$$Q_I^T - Q_M^T = Q_{\mathrm{latent}}^T. \qquad (2)$$

Holland & Jenkins, *JPO*, 1999

Heat Flux Parameterization

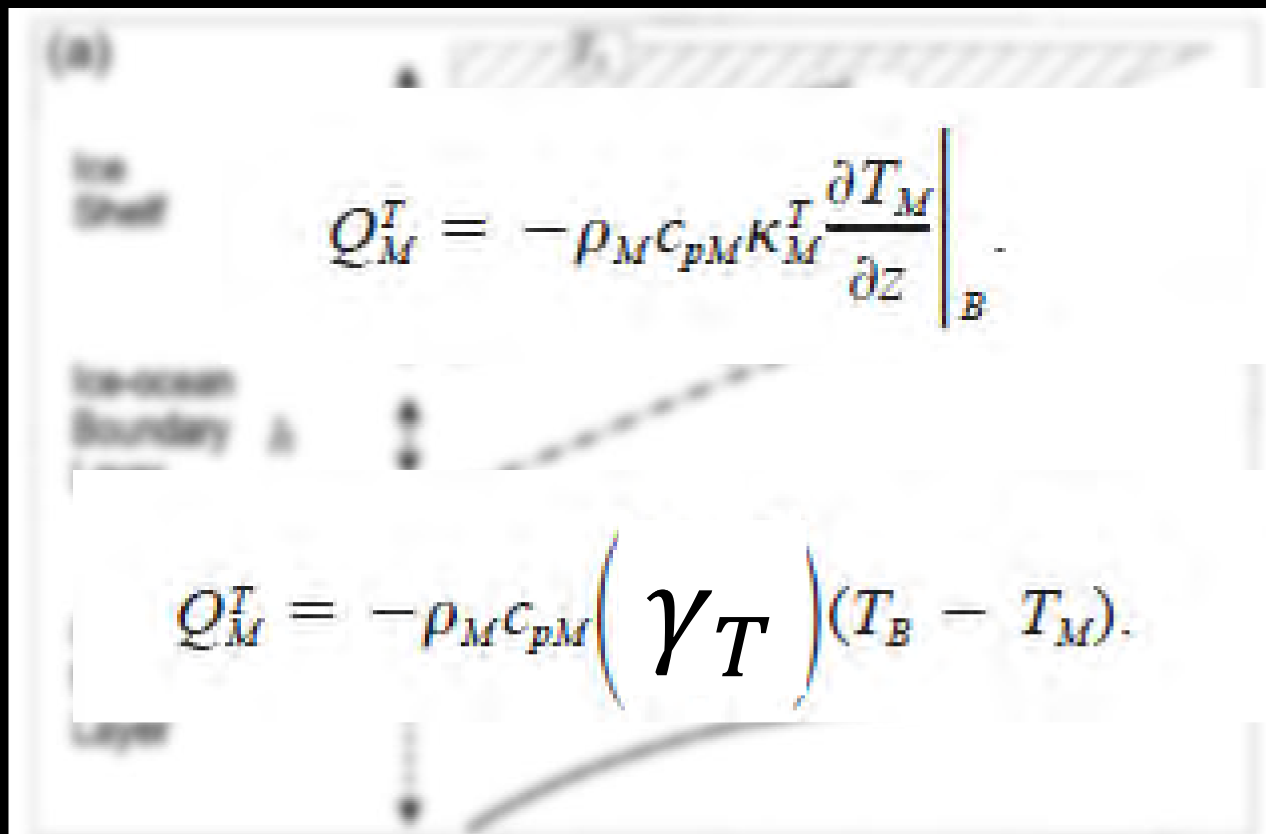

$$Q_M^T = -\rho_M c_{pM} \kappa_M^T \left.\frac{\partial T_M}{\partial z}\right|_B . \qquad (7)$$

$$Q_M^T = -\rho_M c_{pM} \left(\gamma_T \right) (T_B - T_M). \qquad (9)$$

Holland & Jenkins, *JPO*, 1999

Salt Fluxes

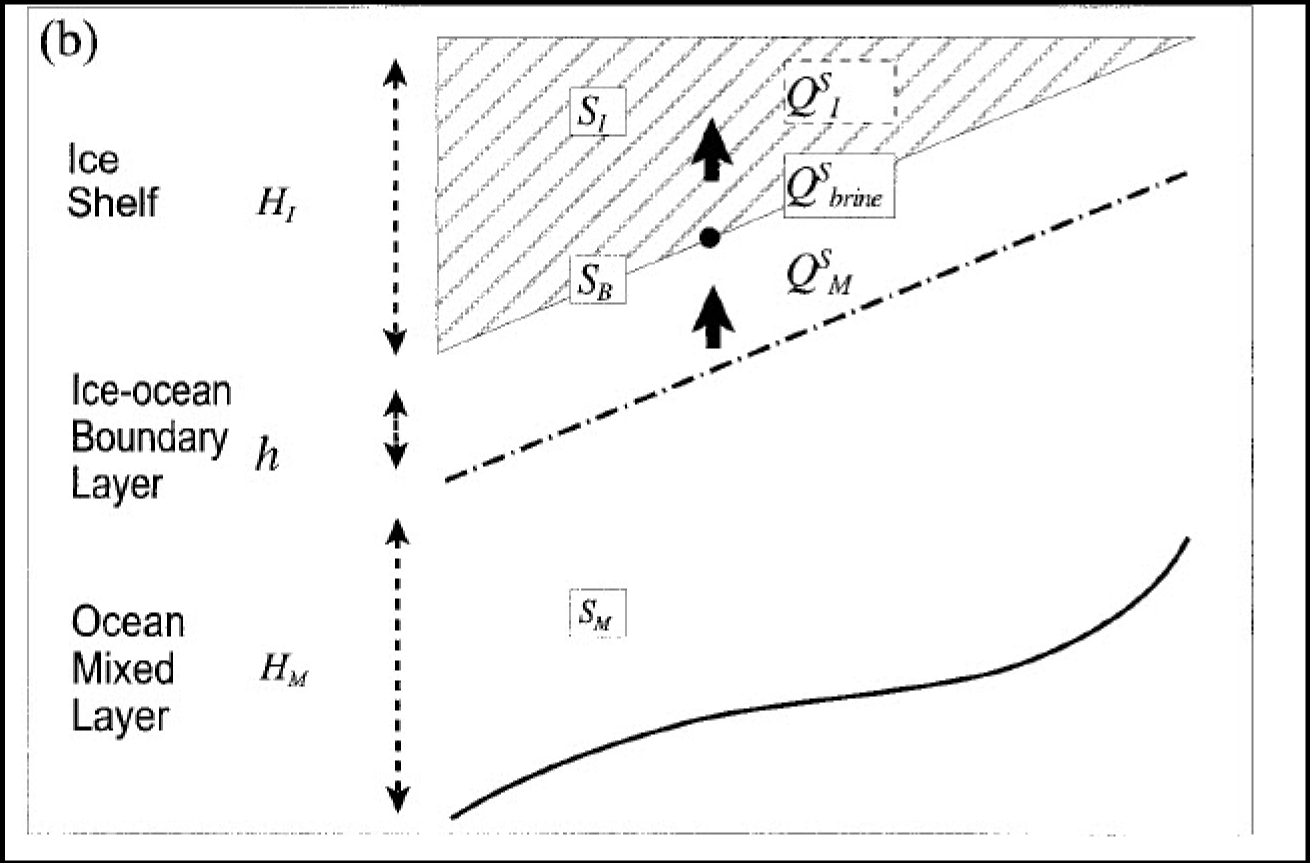

Holland & Jenkins, *JPO*, 1999

'Three-Equation' Formulation

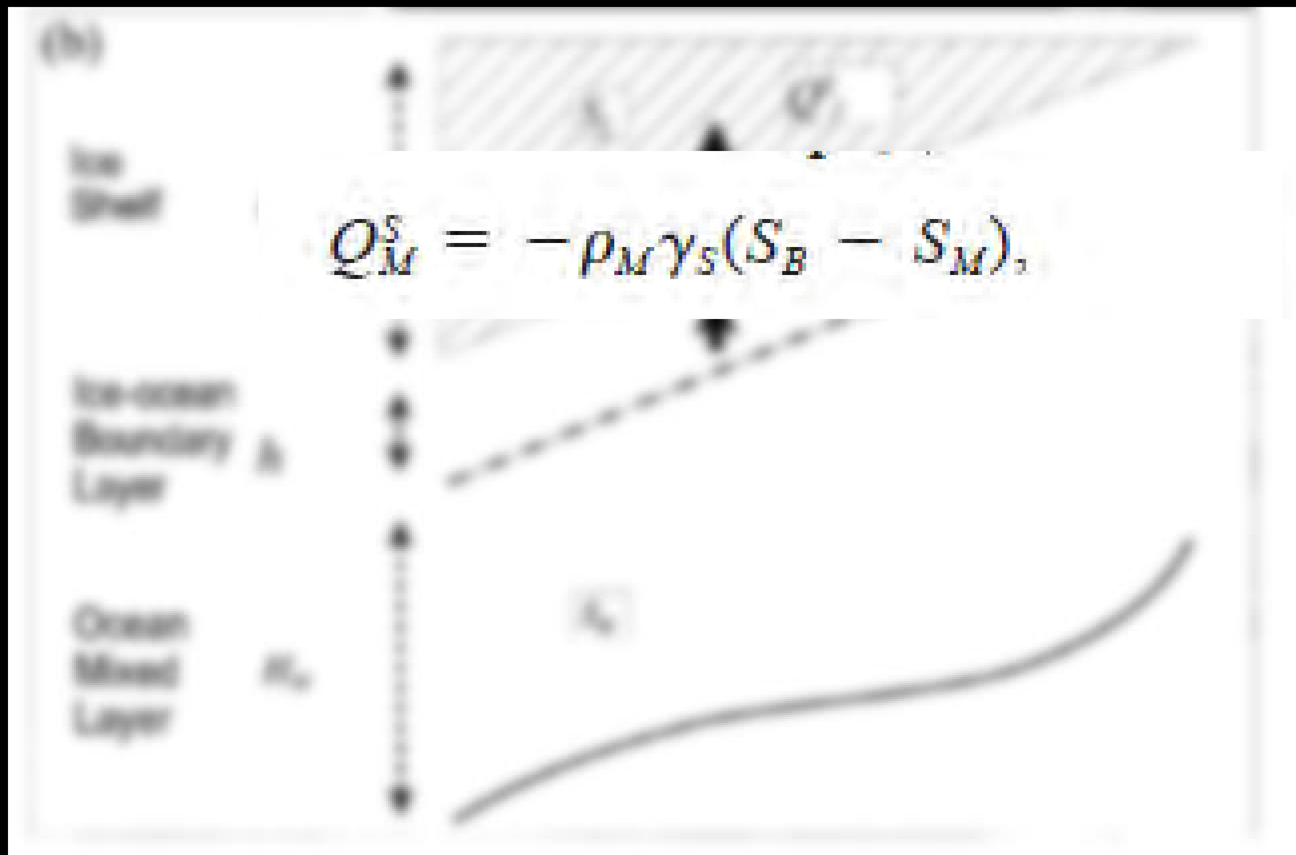

$$Q^S_M = -\rho_M \gamma_S (S_B - S_M), \qquad (10)$$

Holland & Jenkins, *JPO*, 1999

$\gamma_{T,S}$

Exchange Coefficients Parameterization

$$\gamma_{T,S} = \frac{u_*}{\Gamma_{\text{Turb}} + \Gamma_{\text{Mole}}^{T,S}}, \qquad (14)$$

$$\Gamma_{\text{Mole}}^{T,S} = 12.5(\text{Pr}, \text{Sc})^{2/3} - 6. \qquad (16)$$

$$\Gamma_{\text{Turb}} = \frac{1}{k}\ln\left(\frac{u_*\xi_N\eta_*^2}{fh_\nu}\right) + \frac{1}{2\xi_N\eta_*} - \frac{1}{k} \qquad (15)$$

$$\eta_* = \left(1 + \frac{\xi_N u_*}{fL_O R_c}\right)^{-1/2}, \qquad (18)$$

Holland & Jenkins, *JPO*, 1999

Cold Water Interaction:

Classic *Ice Pump*

Ice Pump Circulation: Intrinsic to Mode 1 Waters

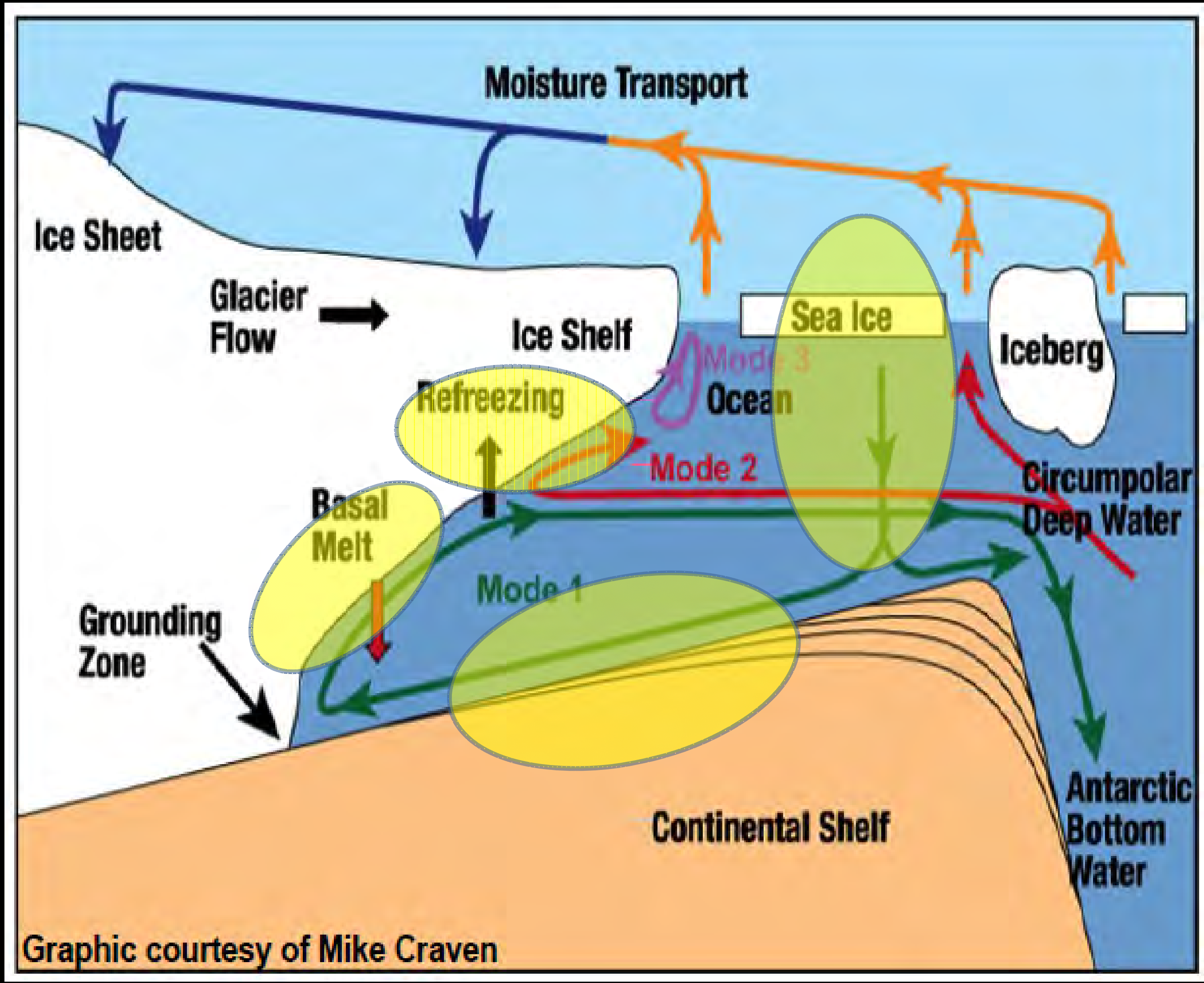

Ice Front Circulation: Intrinsic to Mode 3 Waters

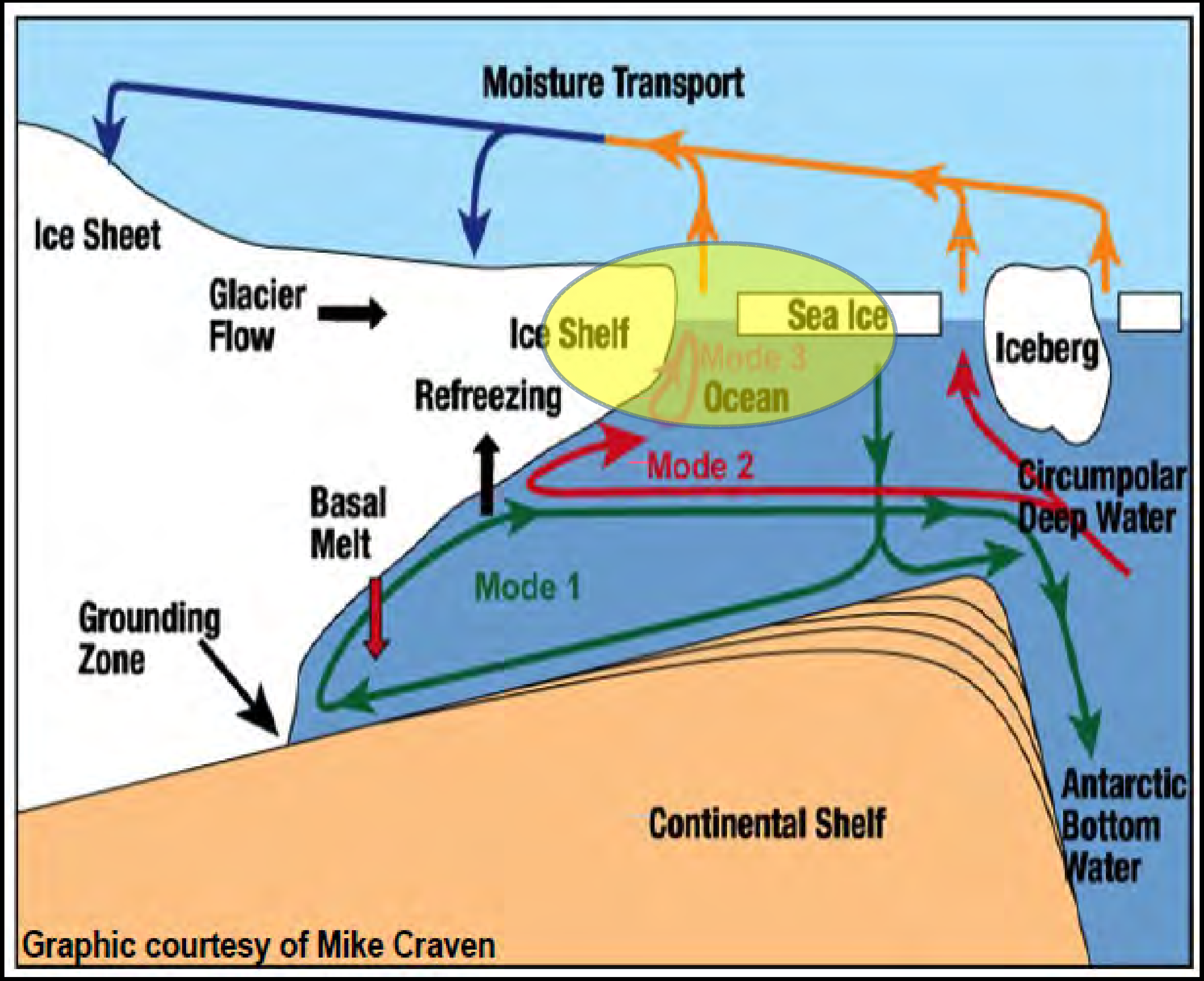

Observations of Mode 3 Interaction

JOURNAL OF GEOPHYSICAL RESEARCH, VOL. ???, XXXX, DOI:10.1029/,

Ir
M
A.
Hc

Abstract. A six month temperature record collected below McMurdo Ice Shelf in 2011-2012 shows the temporal and spatial structure of the summertime warm water signal which penetrates beneath the ice shelf. The strength and duration of the warm water intrusion suggest an annual melt rate at Windless Bight of 0.71m/yr. A Ross Sea numerical model demonstrates a seasonal warm water pathway leading from the west side of the Ross Sea Polynya (RSP) towards McMurdo Sound. The warm water enters McMurdo Sound, subducts beneath the ice shelf and causes accelerated summer melting. Temperature data were recorded using Distributed Temperature Sensing fiber optics, which gives a vertical temperature profile at a one meter vertical resolution. This study constitutes one of the first successful implementations of this technology in polar regions.

Stern et al., *submitted JGR*, 2013

McMurdo Ice Shelf: Windless Bight (WB) Field Site

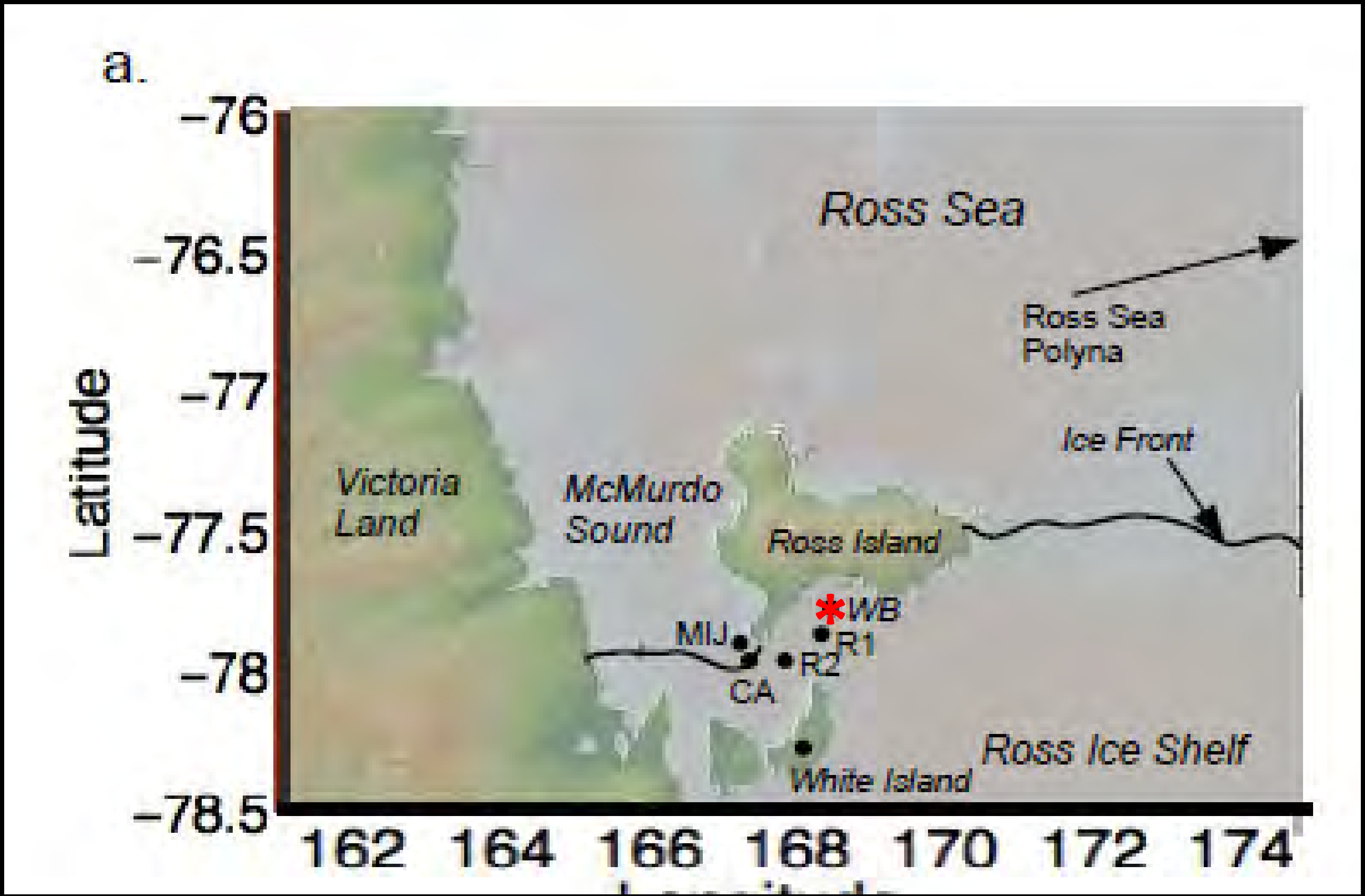

Stern et al., *submitted JGR*, 2013

Modeled Temperatures – McMurdo Ice Shelf

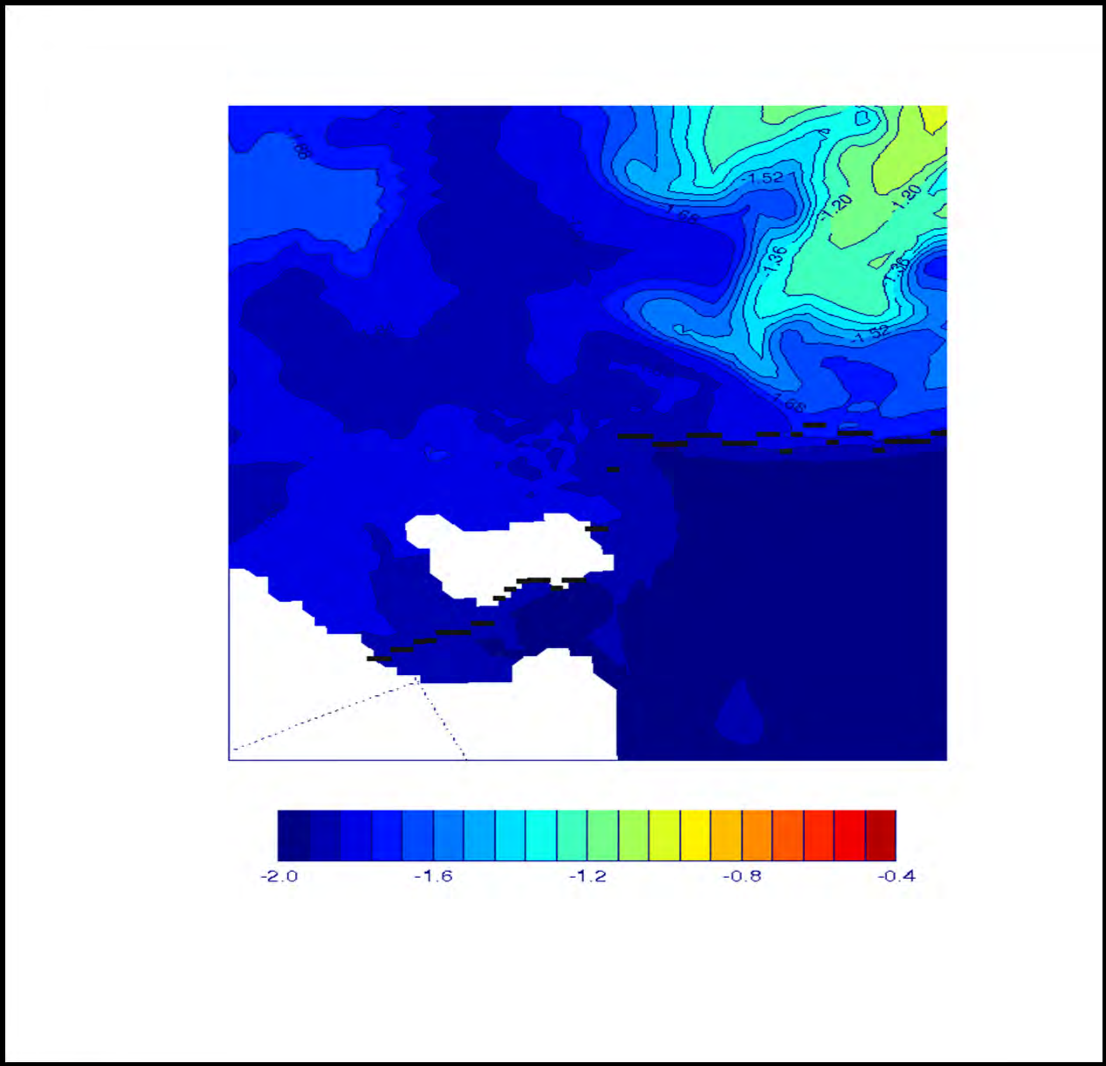

M. Dinniman, ROMS output, 2012

Distributed Temperature Sensing

The Antarctic Sun

"News about the USAP, the Ice, and the People"

Home ▸ Science ▸ Wired

SHARE

Victor Zagorodnov, left, empties snow out of the drill used to core through the ice shelf at Windless Bight, while David Holland prepares for the next flight. The researchers deployed a distributed temperature sensing system to make sustained ocean temperature measurements underneath the ice.

Photo Credit: Vicki Beaver

Wired

Scientists use fiber optics, lasers to measure water temperature below ice

Optical Fiber Installation

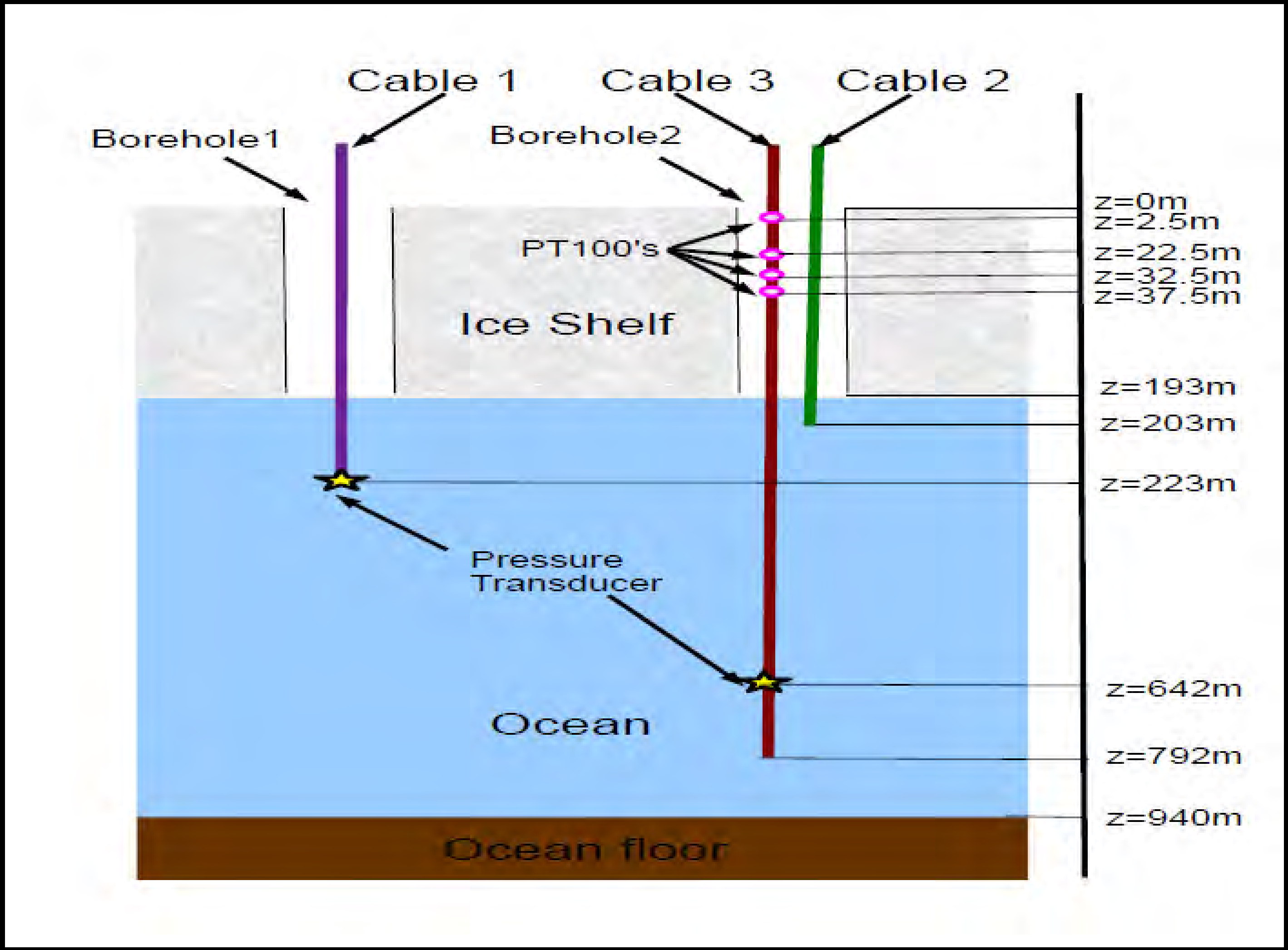

Stern et al., *submitted JGR*, 2013

Year-Long Temperature Profile

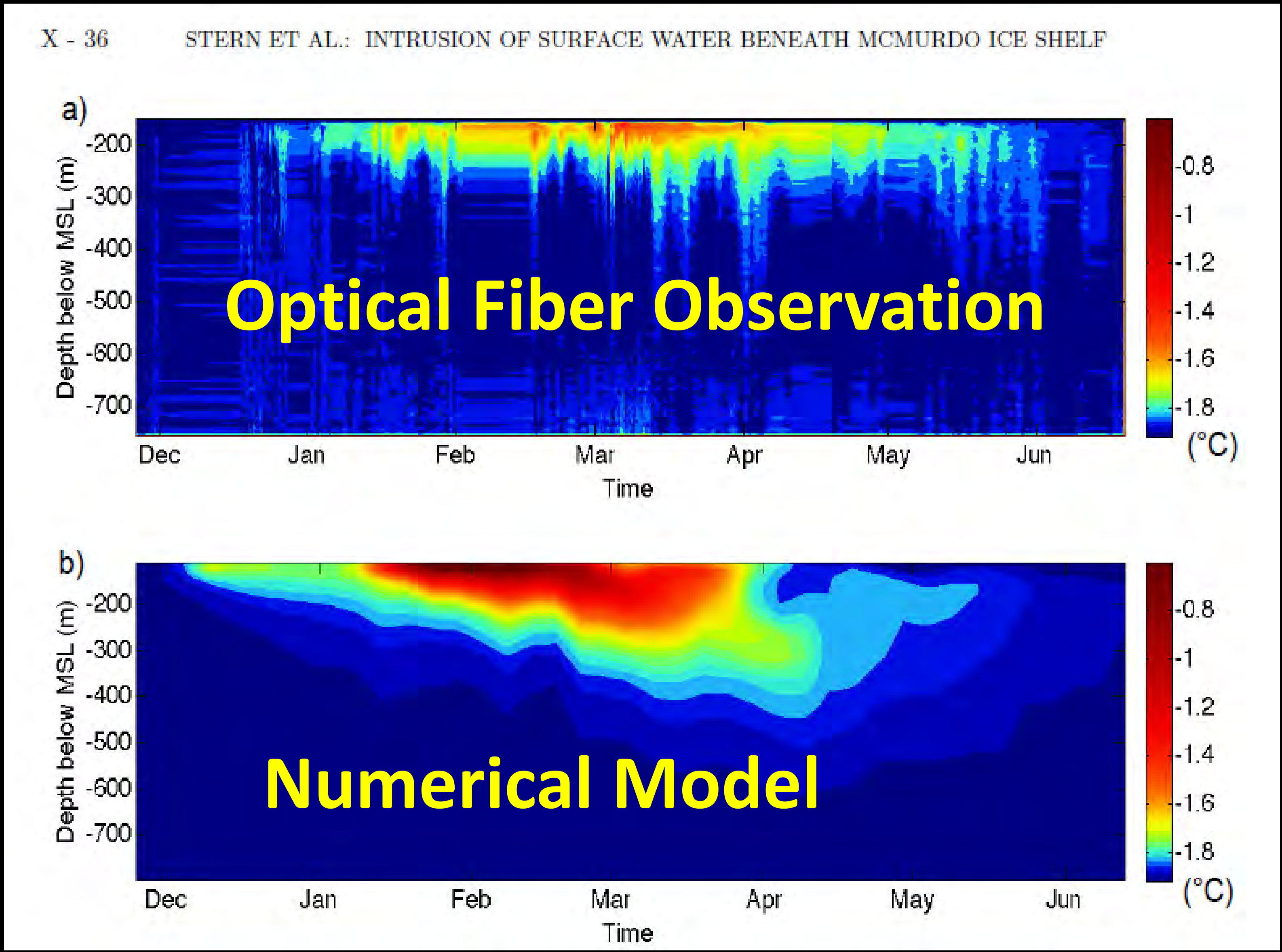

Stern et al., *submitted JGR*, 2013

Melt Rate Estimation: 'Two-Equation' Formulation

$$< w'T' >= w_0 Q_L \quad (1)$$

$$< w'T' >= St_* u_{*0}(T_w - T_f(S_w)) \quad (2)$$

$$w_0 = \frac{\rho_{ice}}{\rho_w}\dot{m}.$$

$$\dot{m} = St_* u_{*0}(T_w - T_f(S_w))\frac{\rho_w}{\rho_{ice}}(Q_L)^{-1} \quad (4)$$

Stern et al., *submitted JGR*, 2013

Melt Rate Comparison: Numerical Model vs. Optical Fibre

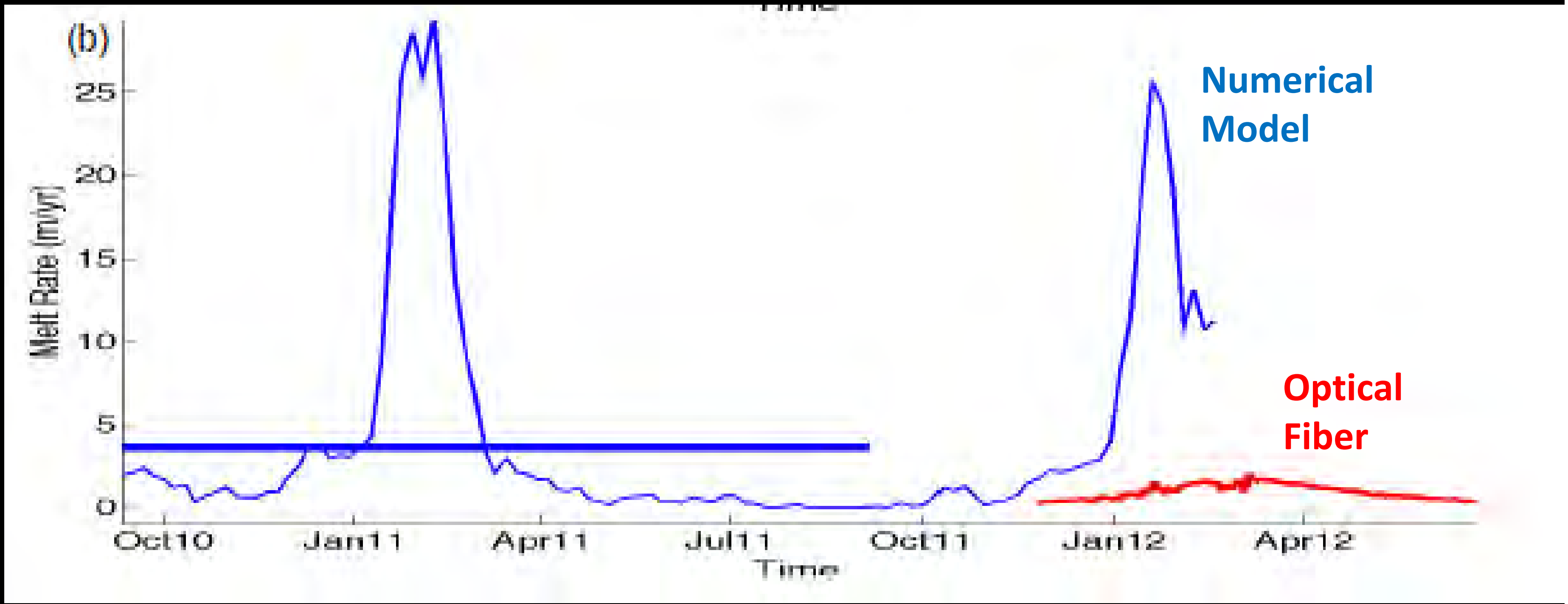

Stern et al., *submitted JGR*, 2013

Sensitivity of Basal Melt Rates: Mode 3 Intrusion

Parameter	Parameter Value	Change in Parameter	Change in Melt Rate
Salinity	34.5psu	0.1psu	0.02m/yr
Mixed Layer Velocity (U_M)	$0.072 ms^{-1}$	$0.01 ms^{-1}$	0.1m/yr
Drag Coefficient (c_d)	1.5×10^{-3}	0.1×10^{-3}	0.02m/yr
Pressure (p)	156db	10db	0.03m/yr
Stanton Number (St_*)	0.0057	0.001	0.12m/yr
Depth below ice shelf base	10m	5m	0.05m/yr

Stern et al., *submitted JGR*, 2013

3

Warm Water Interaction:

Basal Channels

Basal Channelization of PIG: Evident from DEM

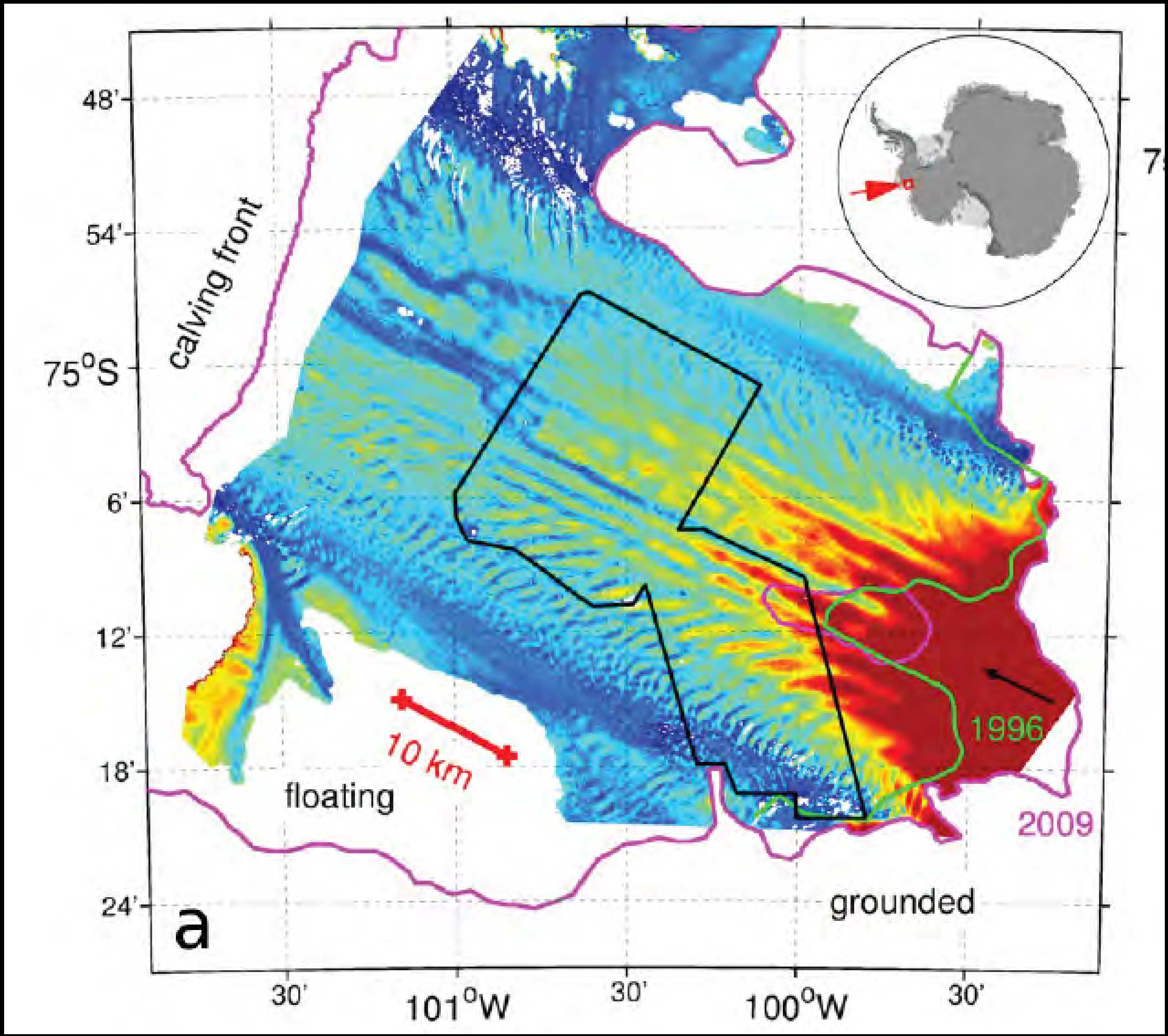

Dutrieux et al., TCD, 2013

Numerical Modeling of Basal Channels

Journal of Glaciology, Vol. 58, No. 212, 2012 doi: 10.3189/2012JoG12J003

Ice-shelf basal channels in a coupled ice/ocean model

Carl V. GLADISH,[1,2] David M. HOLLAND,[2] Paul R. HOLLAND,[3] Stephen F. PRICE[4]

[1]*New York University Abu Dhabi, Abu Dhabi, UAE*
E-mail: cvg222@nyu.edu
[2]*New York University, New York, NY, USA*
[3]*British Antarctic Survey, Natural Environment Research Council, Cambridge, UK*
[4]*Los Alamos National Laboratory, Los Alamos, NM, USA*

ABSTRACT. A numerical model for an interacting ice shelf and ocean is presented in which the ice-shelf base exhibits a channelized morphology similar to that observed beneath Petermann Gletscher's (Greenland) floating ice shelf. Channels are initiated by irregularities in the ice along the grounding line and then enlarged by ocean melting. To a first approximation, spatially variable basal melting seaward of the grounding line acts as a steel-rule die or a stencil, imparting a channelized form to the ice base as it passes by. Ocean circulation in the region of high melt is inertial in the along-channel direction and geostrophically balanced in the transverse direction. Melt rates depend on the wavelength of imposed variations in ice thickness where it enters the shelf, with shorter wavelengths reducing overall melting. Petermann Gletscher's narrow basal channels may therefore act to preserve the ice shelf against excessive melting. Overall melting in the model increases for a warming of the subsurface water. The same sensitivity holds for very slight cooling, but for cooling of a few tenths of a degree a reorganization of the spatial pattern of melting leads, surprisingly, to catastrophic thinning of the ice shelf 12 km from the grounding line. Subglacial discharge of fresh water along the grounding line increases overall melting. The eventual steady state depends on when discharge is initiated in the transient history of the ice, showing that multiple steady states of the coupled system exist in general.

Gladish et al., J. Glaciology, 2012

Basal Channel Numerical Model:

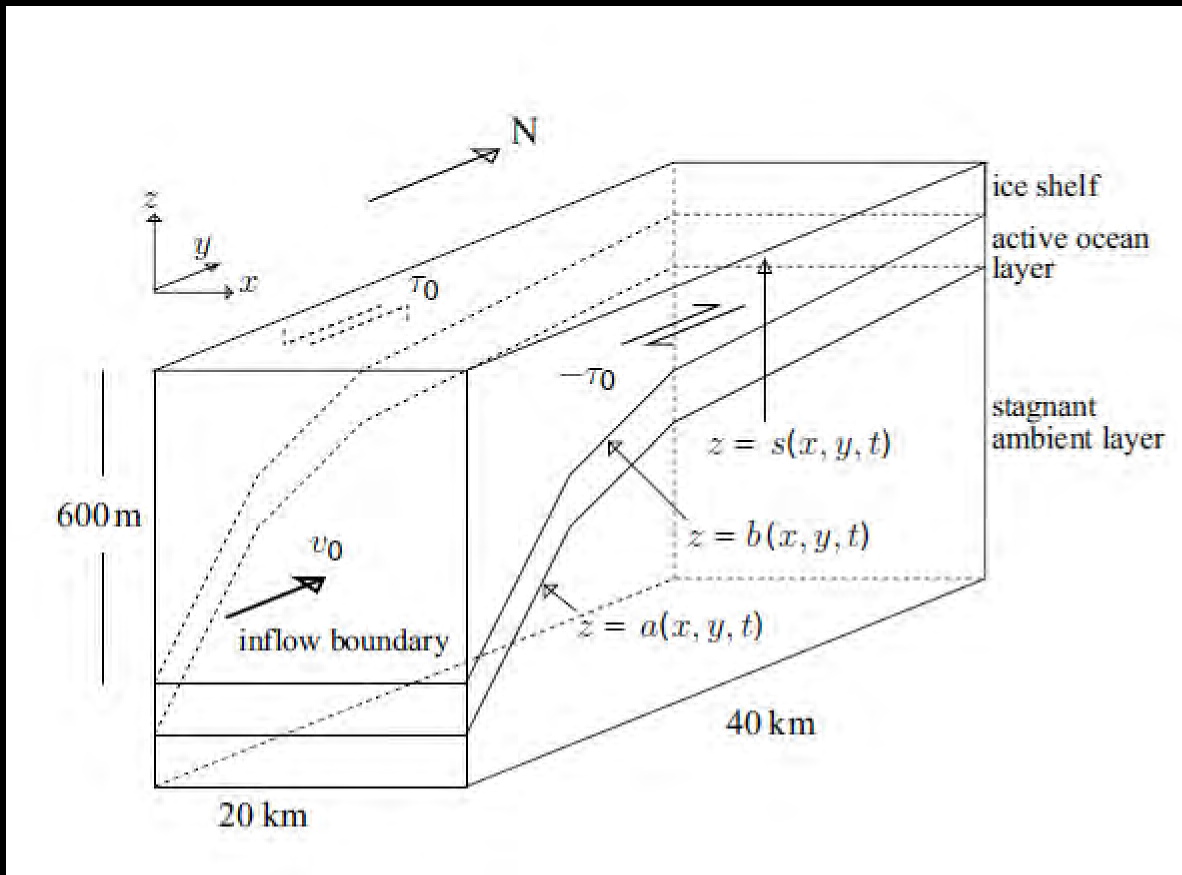

Gladish et al., J. Glaciology, 2012

'Three-Equation' Basal Melt Formulation

$$T_b = \alpha S_b + \beta + \lambda b, \tag{15}$$

$$\rho_o c_o \gamma_T (T - T_b) = \dot{m} \rho_I \mathcal{L} + \dot{m} \rho_I c_I (T_b - T_I) \tag{16}$$

$$\gamma_S (S - S_b) = \dot{m} S_b. \tag{17}$$

$$\gamma_T = \frac{U_*}{2.12 \log(U_* D / \nu_0) + 12.5 Pr^{2/3} - 9} \tag{18}$$

$$\gamma_S = \frac{U_*}{2.12 \log(U_* D / \nu_0) + 12.5 Sc^{2/3} - 9}, \tag{19}$$

Gladish et al., J. Glaciology, 2012

Simulation of Basal Channels

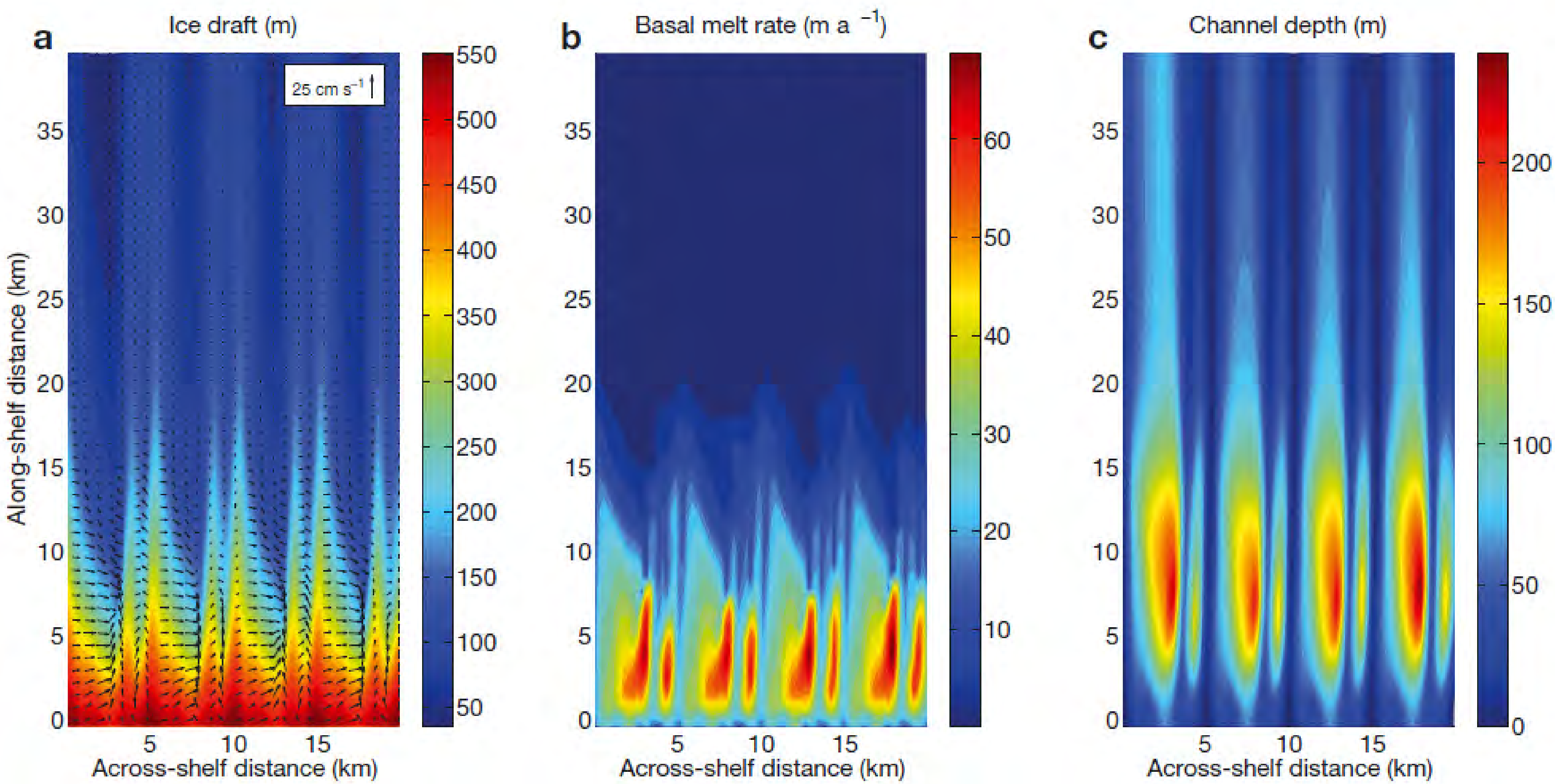

Gladish et al., J. Glaciology, 2012

Planned Observations of Channelized Basal Melting @ PIG

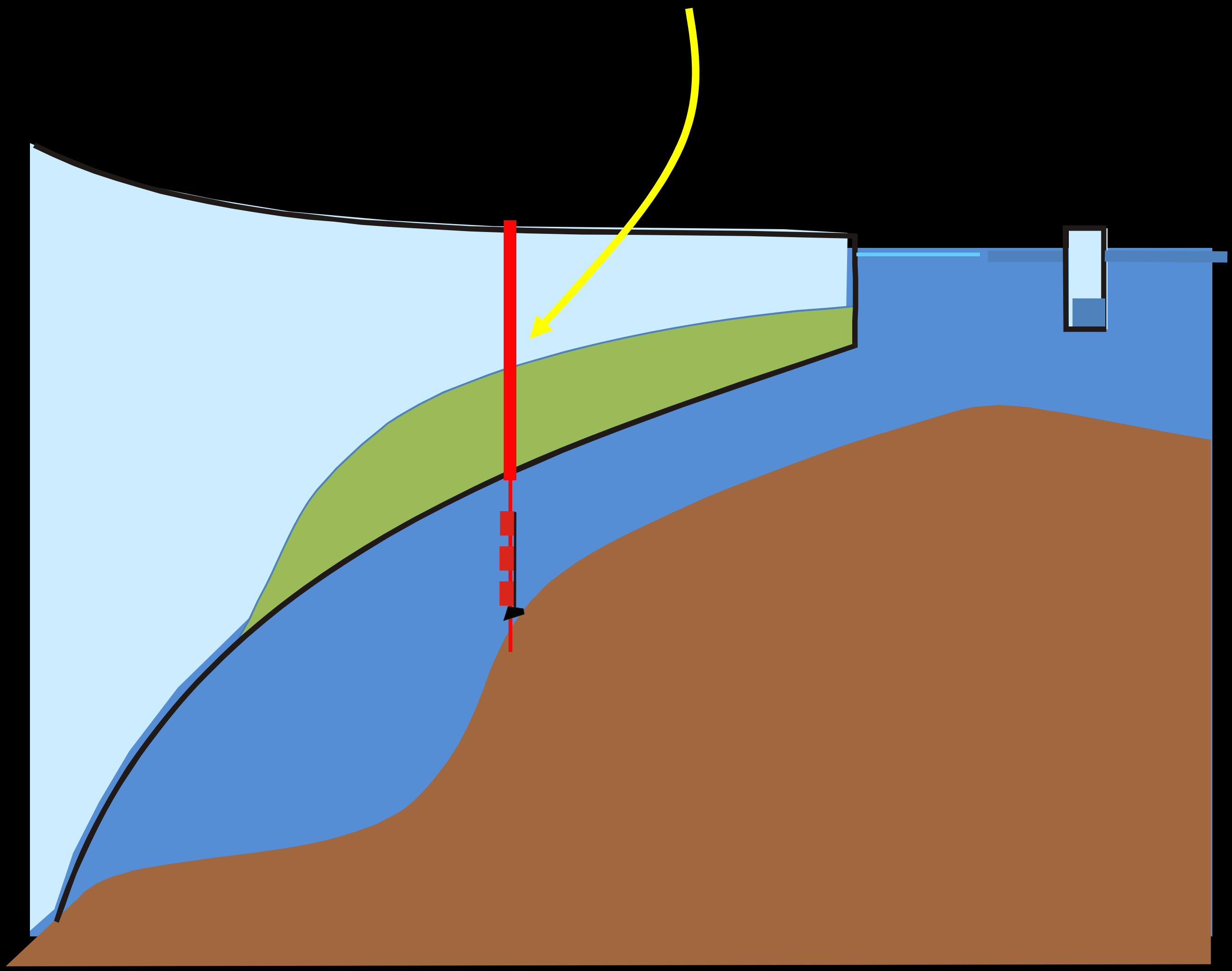

Getting to PIG

PIG Drill Sites:
A, B, C, during Jan 2013

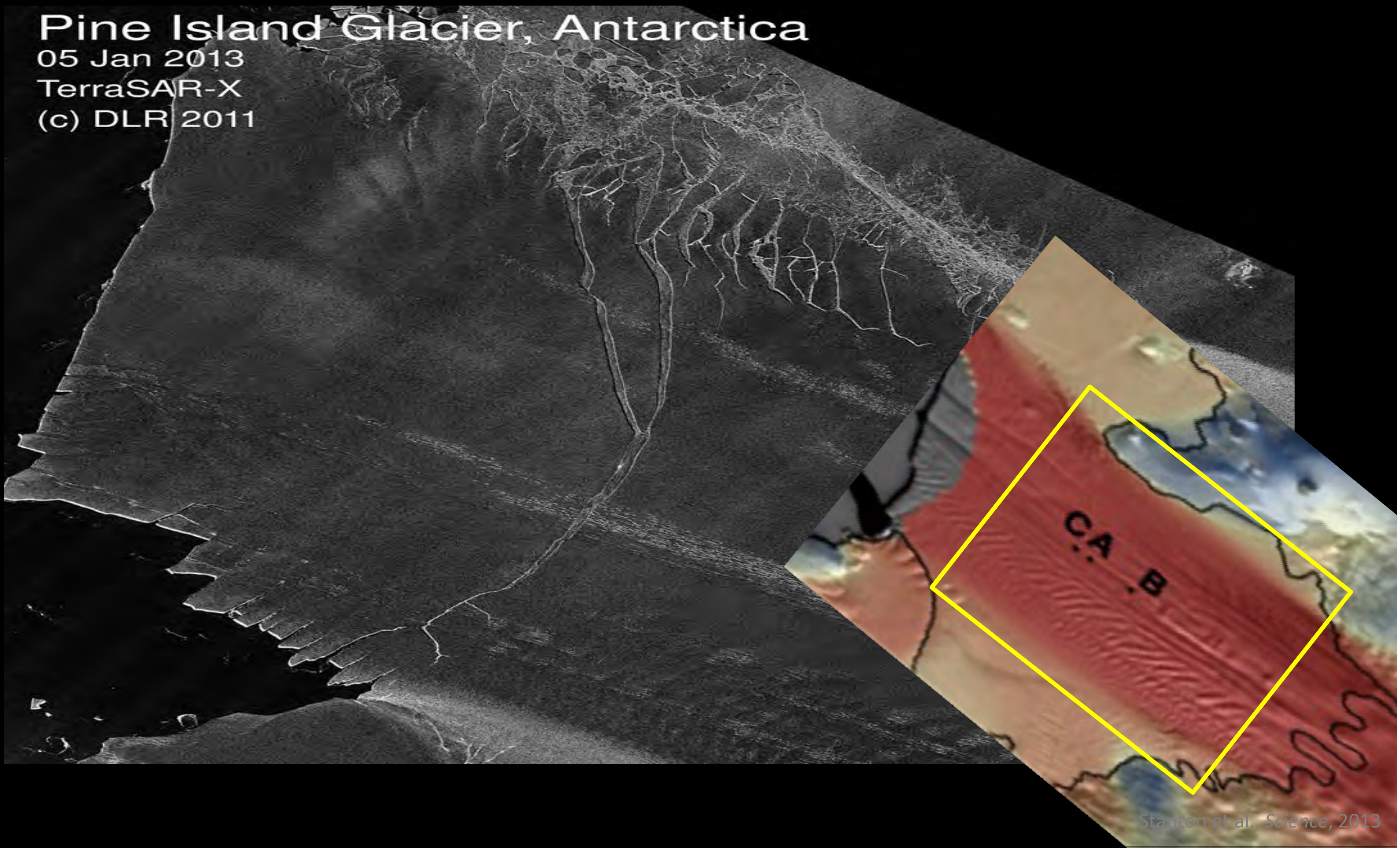

PIG Logistics:
Helicopter Luggage, Jan 2013

Observations of Melt-Rate Related Quantities @ PIG

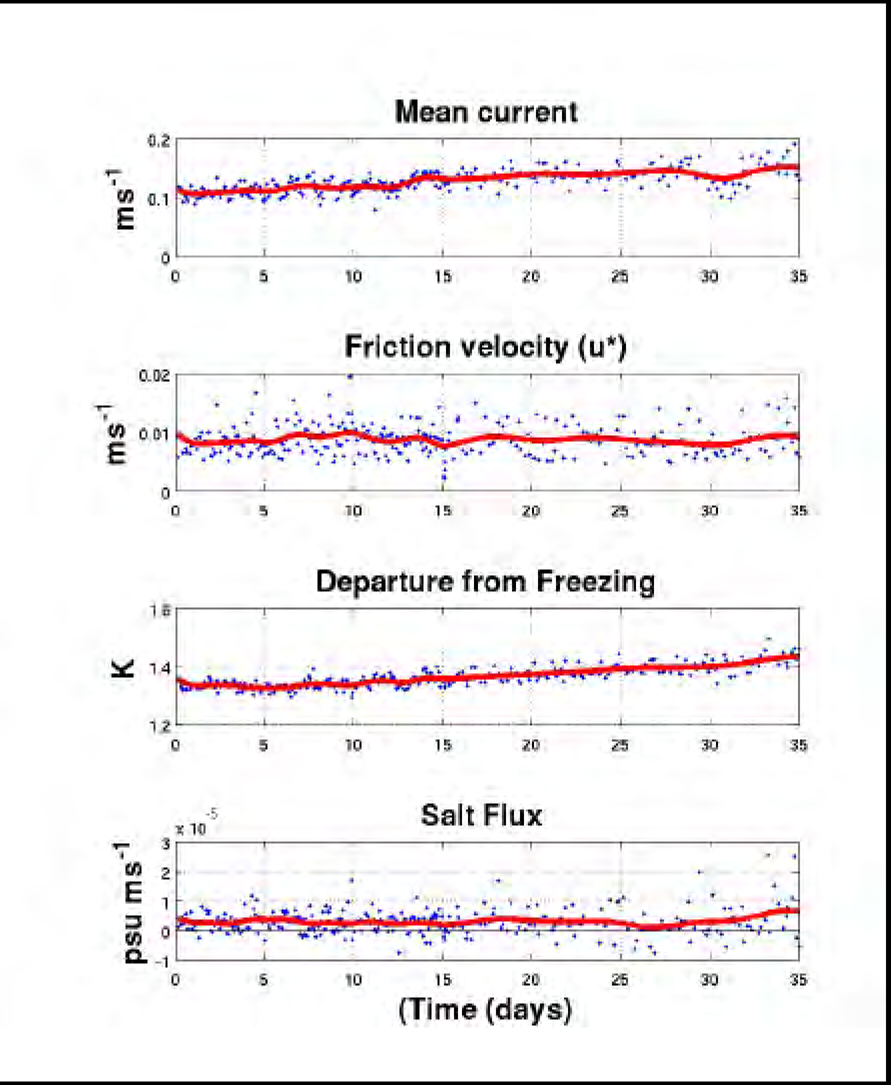

Stanton et al., *Science*, 2013

Comparison Observational and Modelled Basal Melt Rates @ PIG

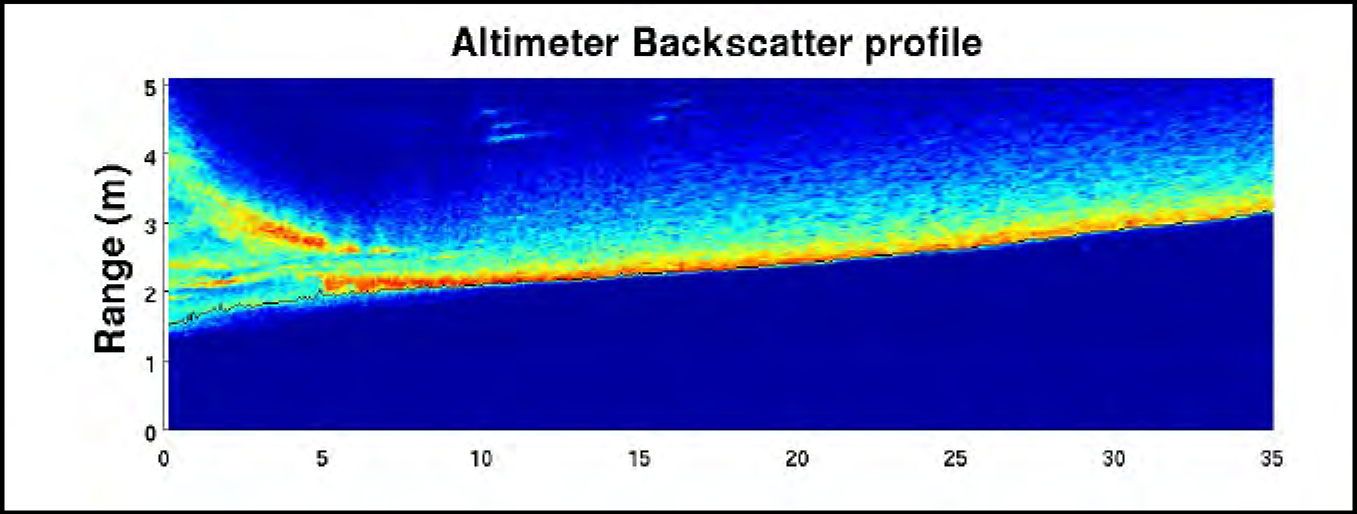

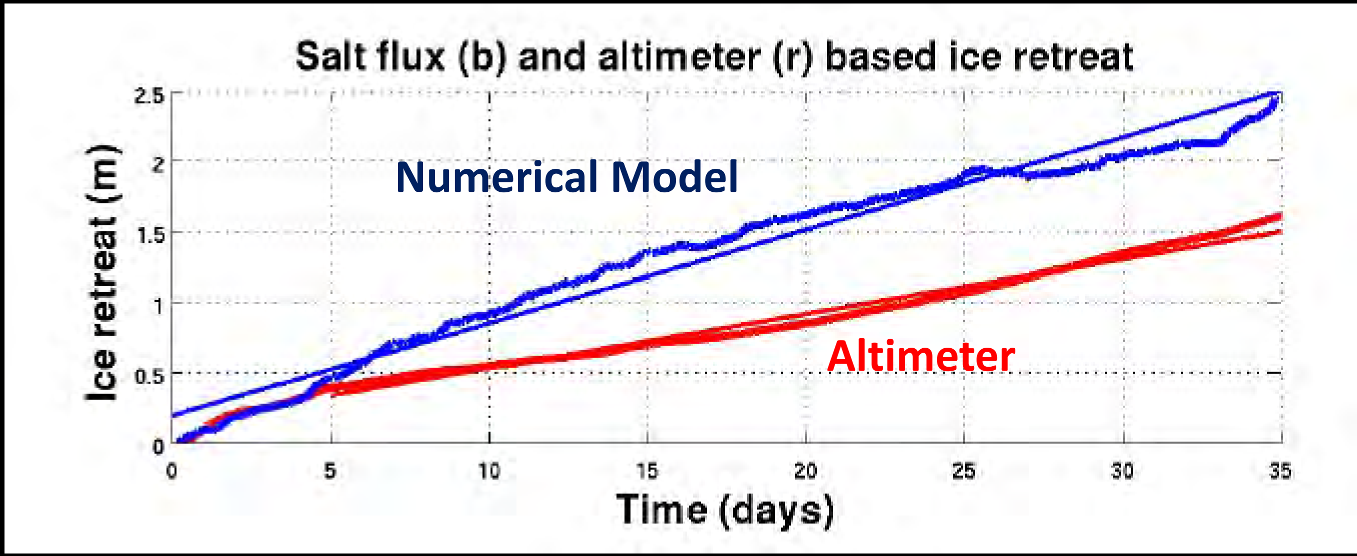

Stanton et al., *Science*, 2013

Glacial Water Interaction:

Fjord Flushing

Virtual Fly-In to Jakobshavn

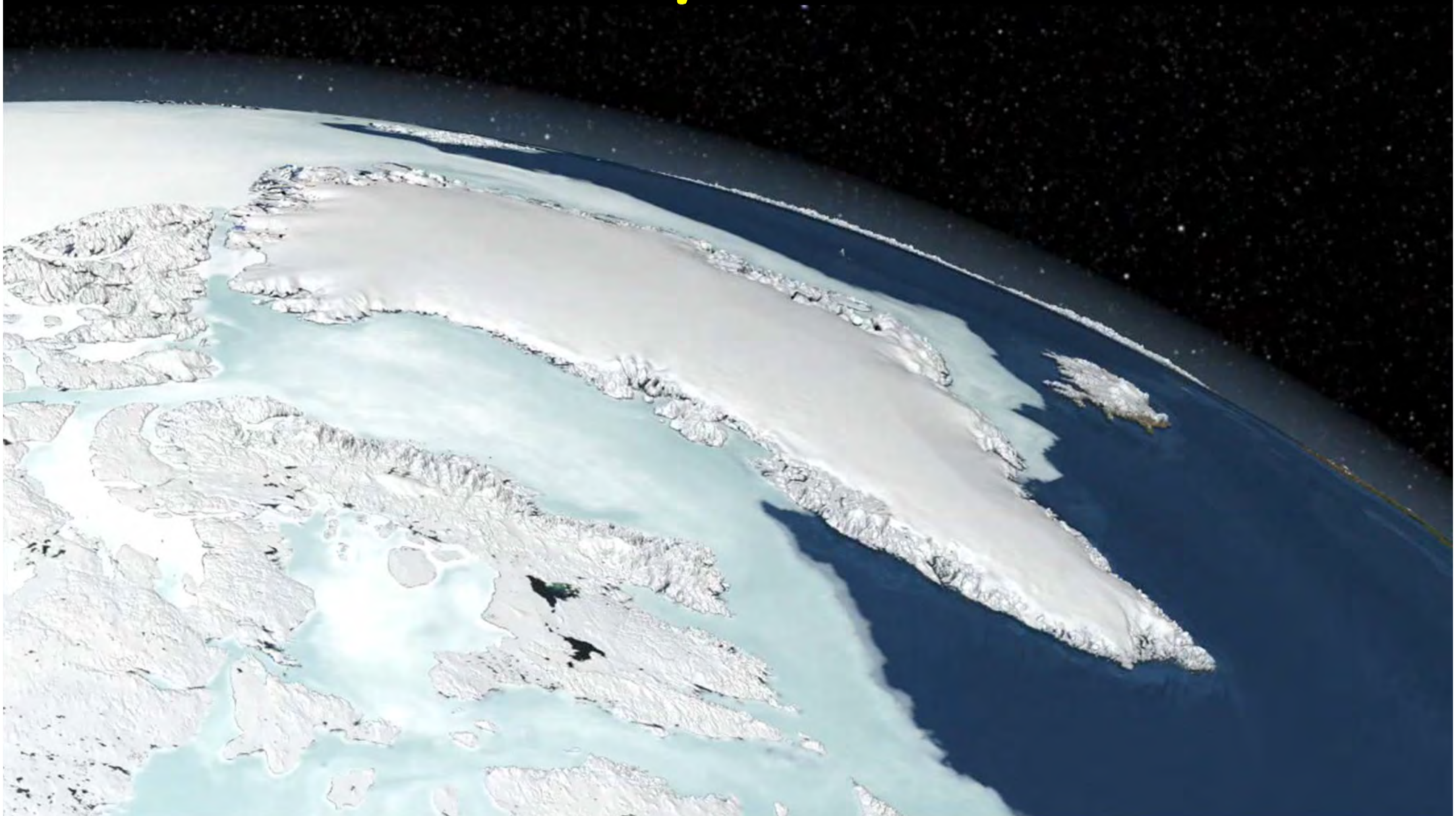

NASA

Boat-based CTD Survey: *Fjord Mouth*

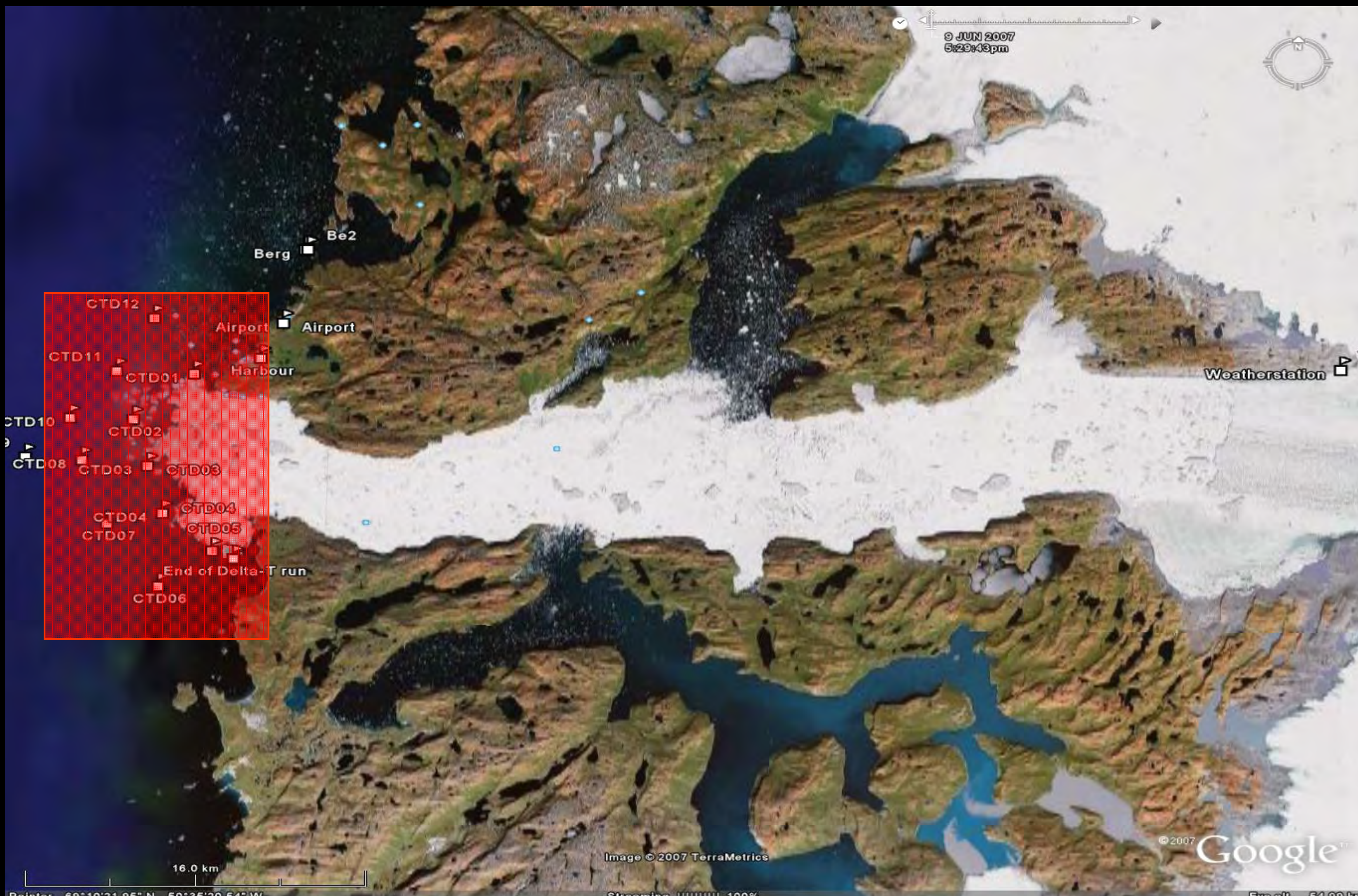

Boat-based CTD Survey: *Fjord Mouth*

CTD Timeseries: *Moorings*

Airborne Temperature Probe: *Target Drop Location*

Airborne Temperature Probe:

Airborne XCP Probe:

Alternate Approach: *Tagged Seals*

Seal Tagging, Greenland
Environmental Monitoring Stations (EMS)
(EFDL)

al tagged with SMRU CTD during August, 2010, near Cape Farewell, S
r high-res version; Photo: Aqqalu Rosing-Asvid.)

Alternate Approach: *Tagged Seals*

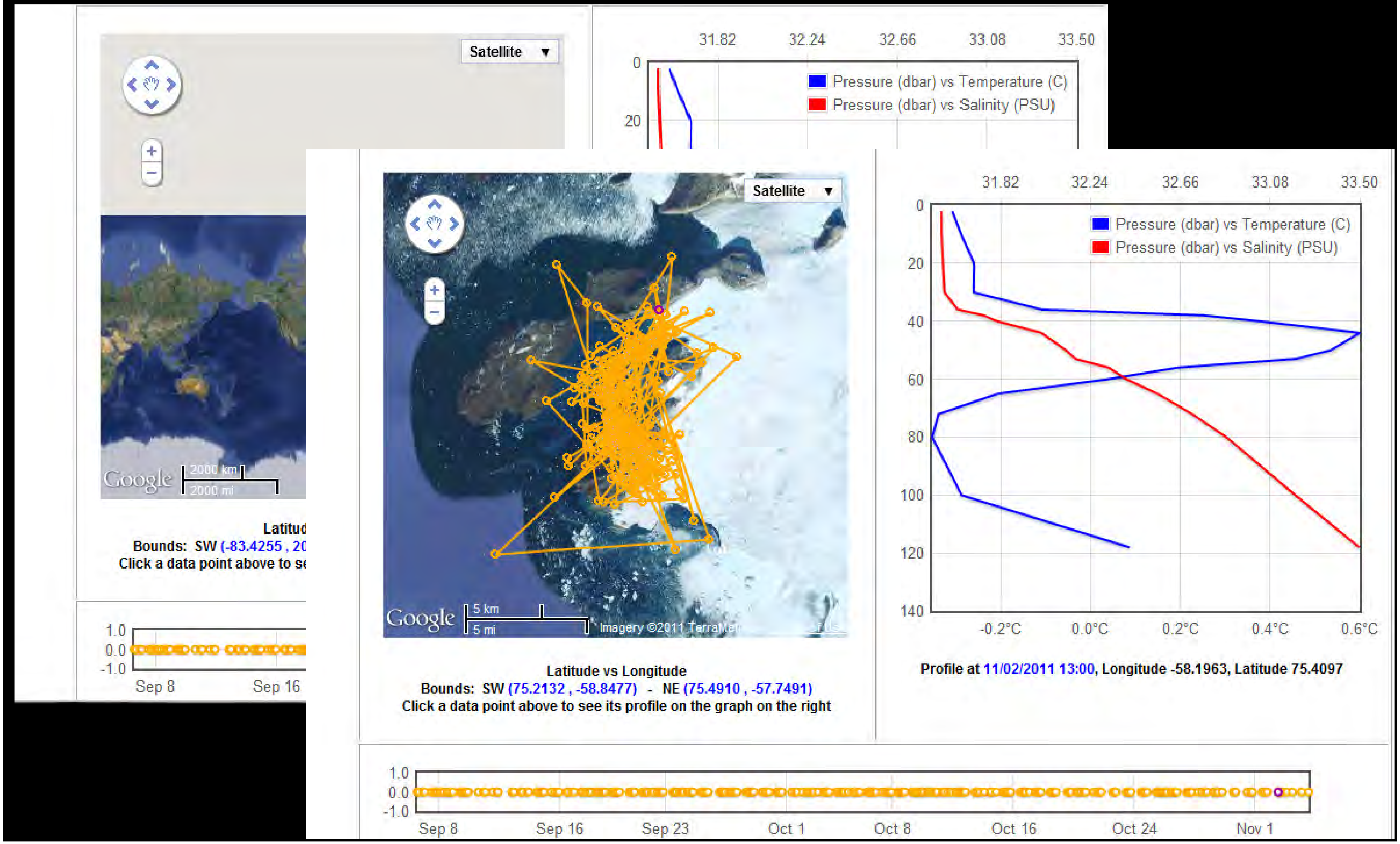

Three-Year Observational Record

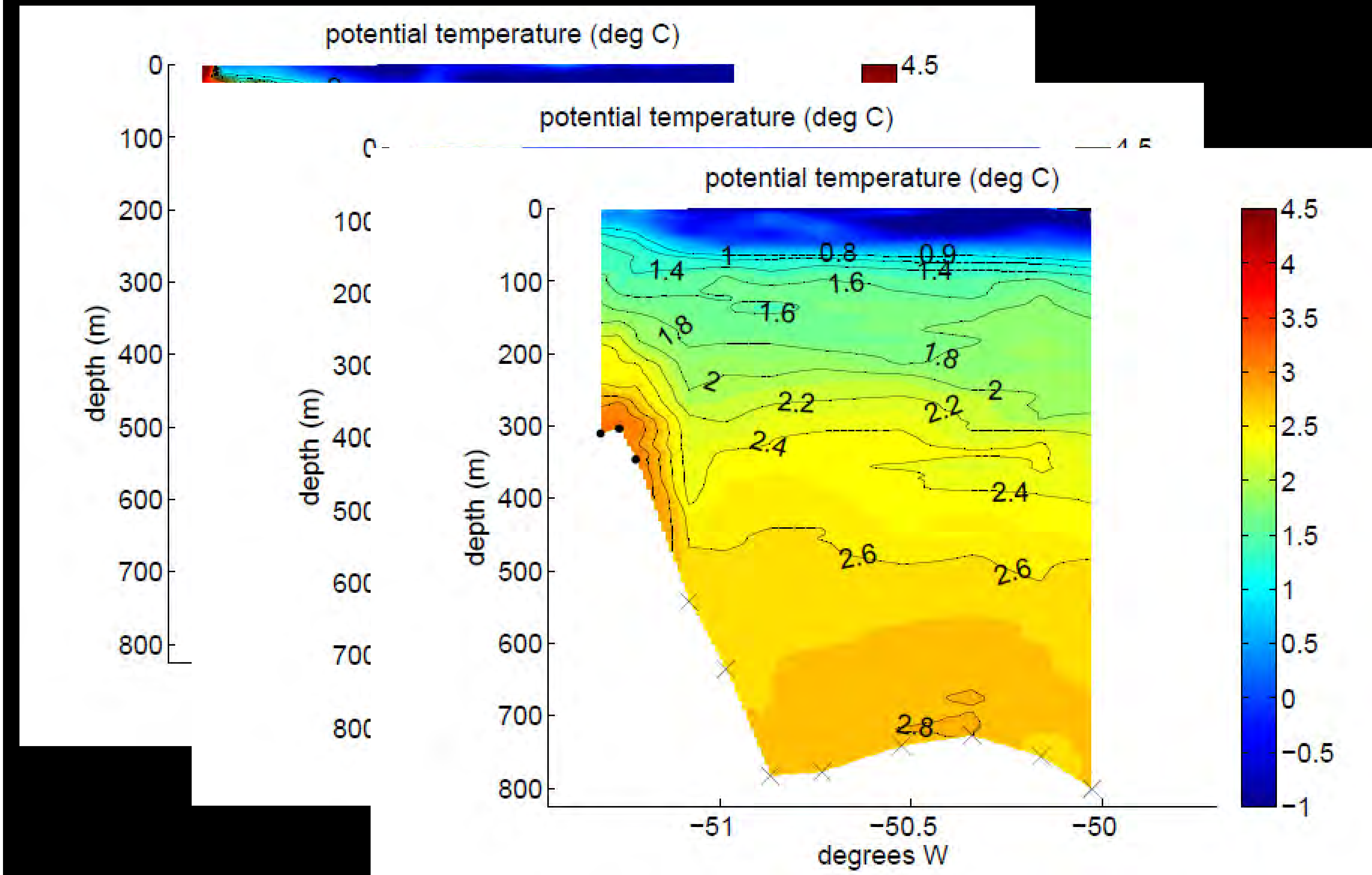

Gladish et al, in prep. , 2013

Ocean-Ice Fjord Model: *MITgcm*

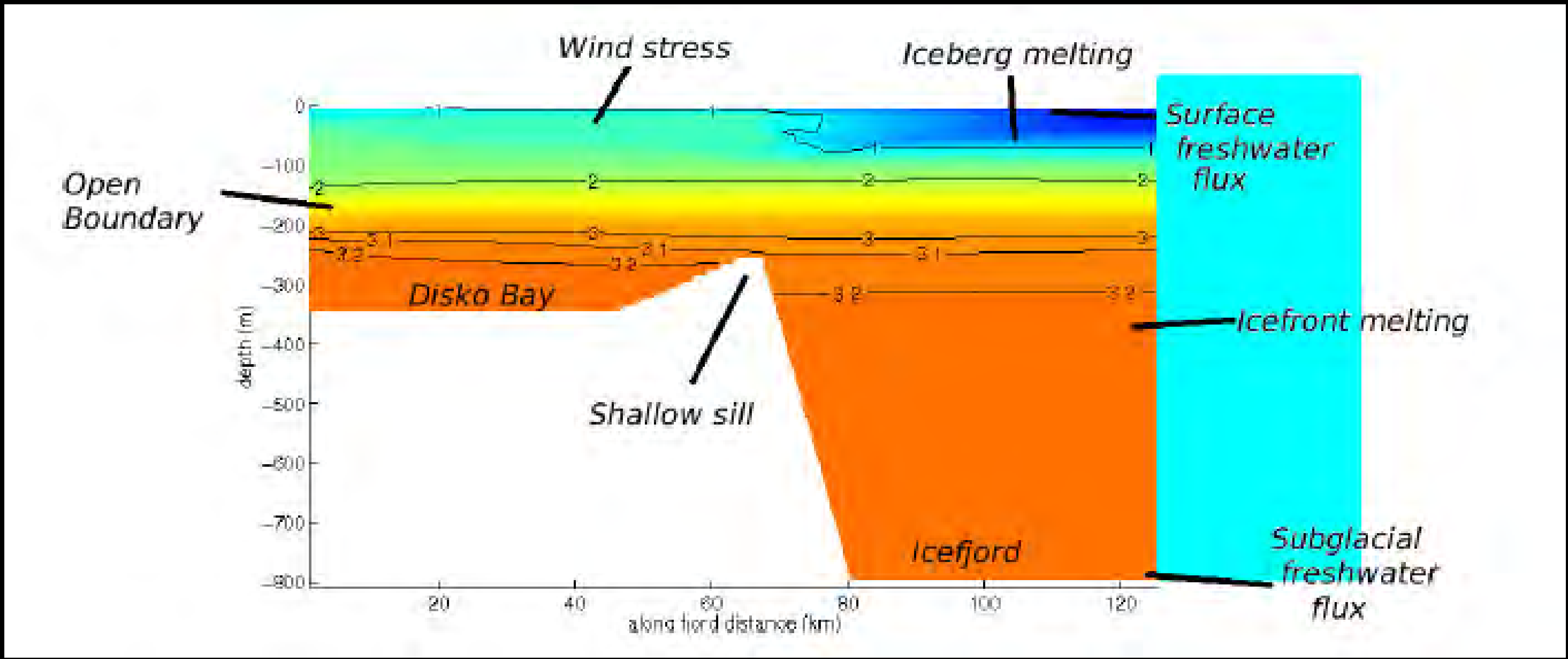

Gladish et al, in prep. , 2013

Numerical Simulation: *Fjord Flushing*

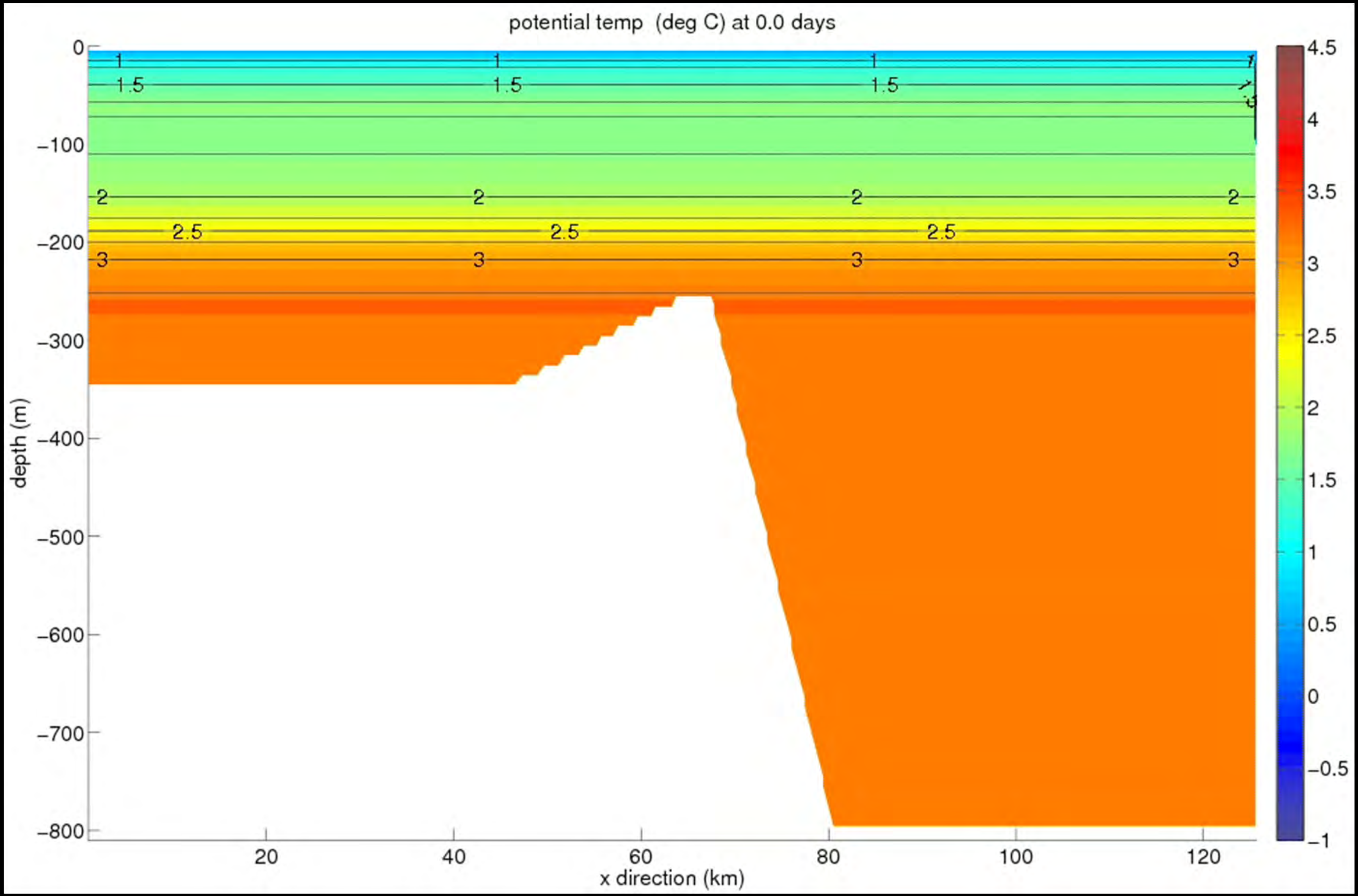

Gladish et al, in prep. , 2013

5

Summary

Ocean-Ice Interactions

Basal Melting:

Cold Water - Classic Ice Pump
Warm Water – Basal Channels
Glacial Water – Fjord Flushing

Ice-Front Calving:

Weak theoretical and observational foundation